Lapo Boschi

Eidgenössische Technische Hochschule Zürich
Swiss Federal Institute of Technology Zurich

open questions in mantle dynamics: contributions from seismic Earth mapping

with Thorsten Becker (USC)

Geochemistry, Seismology, Geodynamics

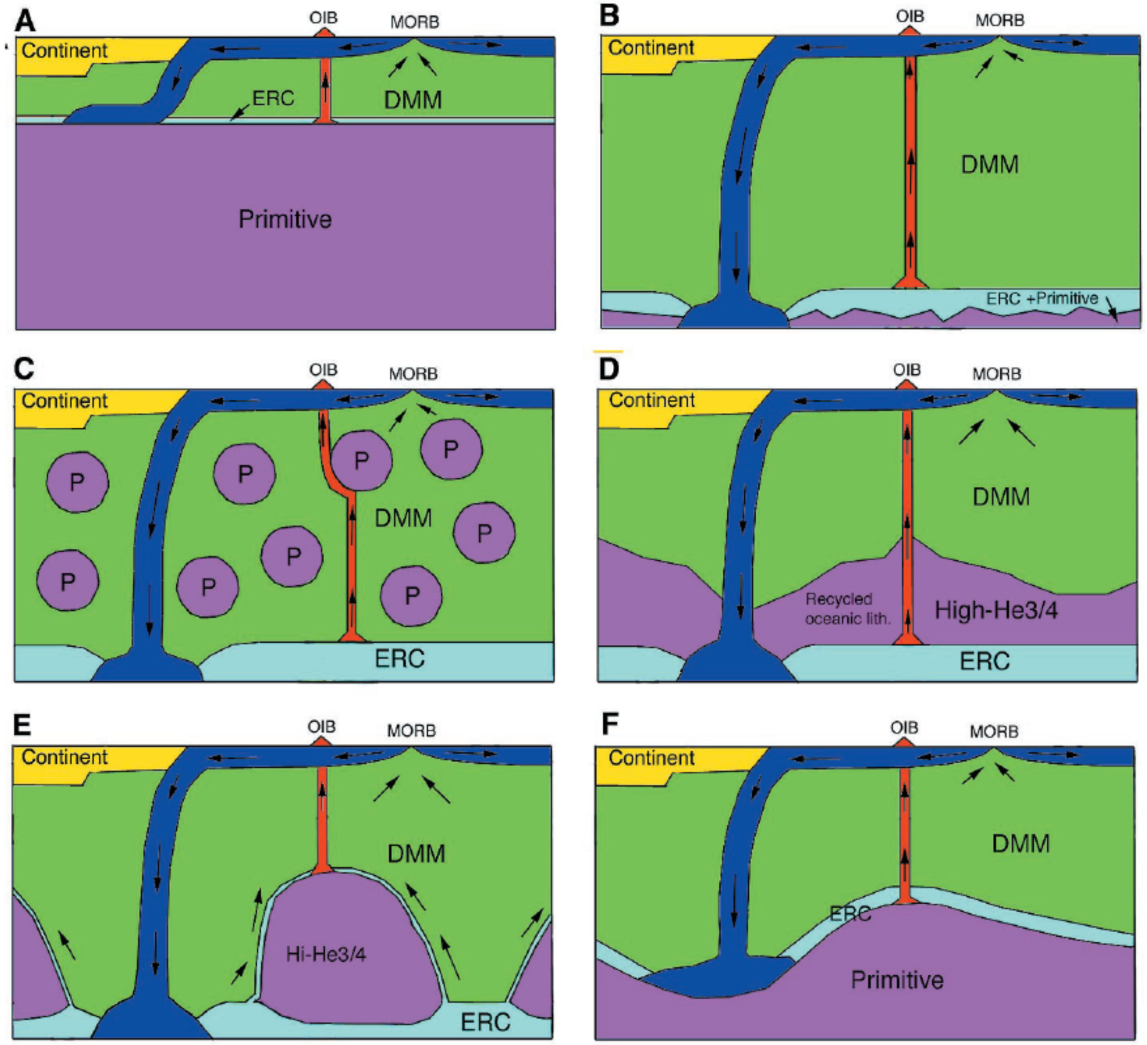

Fig. 2. Some possible locations of mantle reservoirs and relationship to mantle dynamics. Convective features: blue, oceanic plates/slabs; red, hot plumes. Geochemical reservoirs: dark green, DMM; purple, high $^{3}He/^{4}He$ ("primitive"); light green, enriched recycled crust (ERC). (**A**) Typical geochemical model layered at 660 km depth (*7*). (**B**) Typical geodynamical model: homogeneous except for some mixture of ERC and primitive material at the base. (**C**) Primitive blob model (*71*) with added ERC layer. (**D**) Complete recycling model (*83, 84*). (**E**) Primitive piles model [developed from (*85*)]. (**F**) Deep primitive layer (*86*).

Tackley 2000

Geochemistry, Seismology, Geodynamics

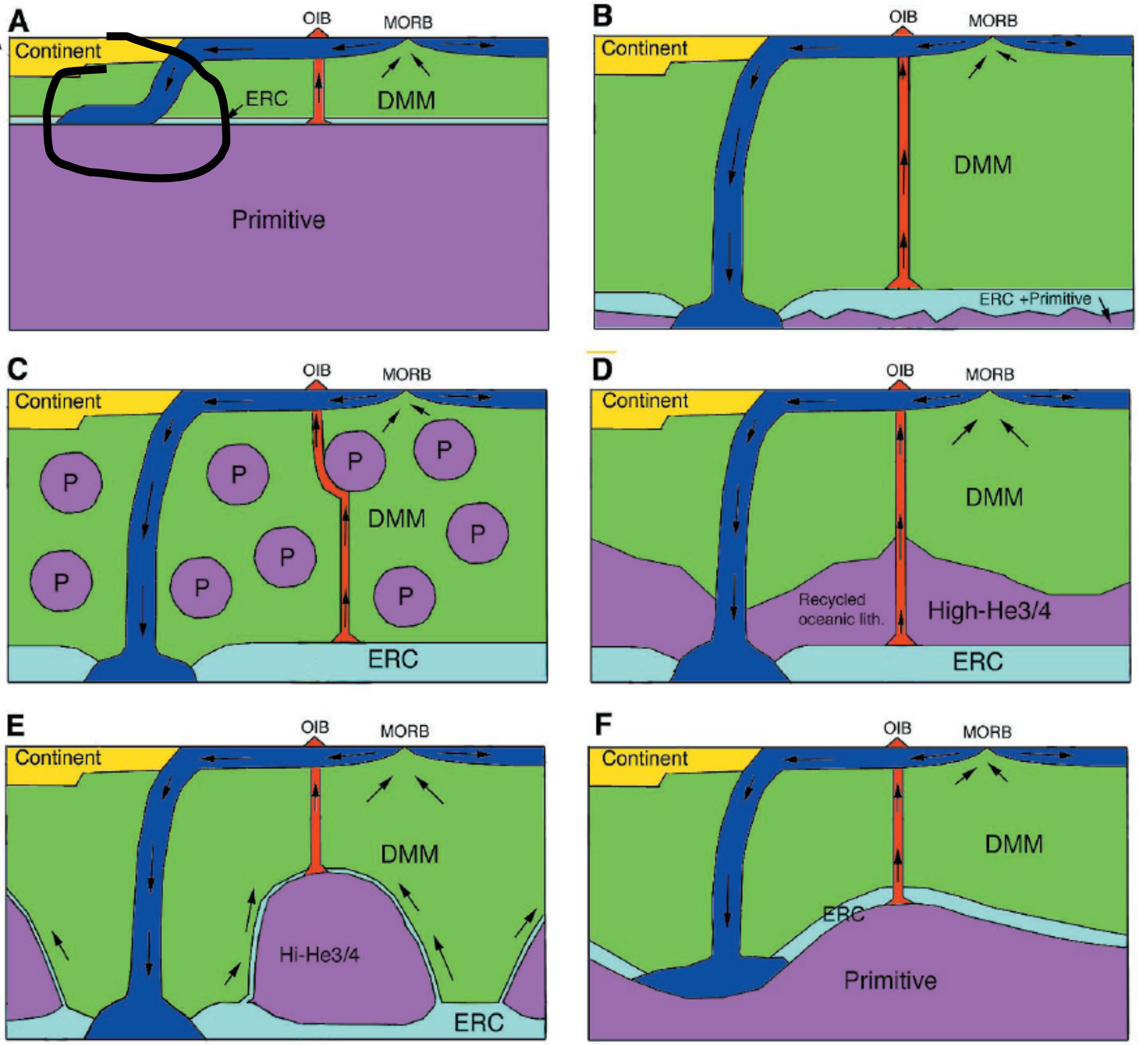

Fig. 2. Some possible locations of mantle reservoirs and relationship to mantle dynamics. Convective features: blue, oceanic plates/slabs; red, hot plumes. Geochemical reservoirs: dark green, DMM; purple, high $^3He/^4He$ ("primitive"); light green, enriched recycled crust (ERC). (**A**) Typical geochemical model layered at 660 km depth (*7*). (**B**) Typical geodynamical model: homogeneous except for some mixture of ERC and primitive material at the base. (**C**) Primitive blob model (*71*) with added ERC layer. (**D**) Complete recycling model (*83, 84*). (**E**) Primitive piles model [developed from (*85*)]. (**F**) Deep primitive layer (*86*).

Tackley 2000

Geochemistry, Seismology, Geodynamics

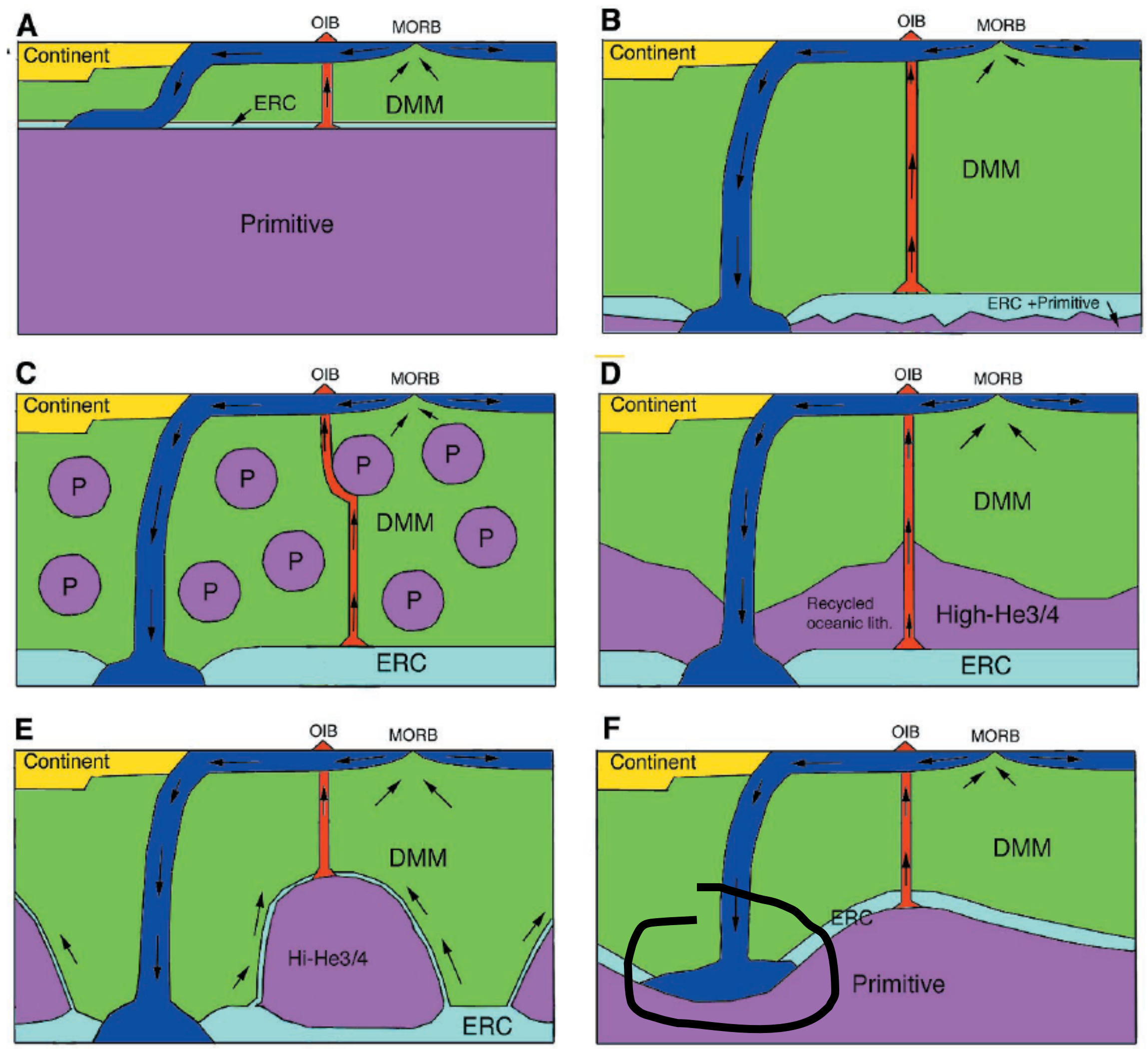

Fig. 2. Some possible locations of mantle reservoirs and relationship to mantle dynamics. Convective features: blue, oceanic plates/slabs; red, hot plumes. Geochemical reservoirs: dark green, DMM; purple, high $^3He/^4He$ ("primitive"); light green, enriched recycled crust (ERC). (**A**) Typical geochemical model layered at 660 km depth (*7*). (**B**) Typical geodynamical model: homogeneous except for some mixture of ERC and primitive material at the base. (**C**) Primitive blob model (*71*) with added ERC layer. (**D**) Complete recycling model (*83, 84*). (**E**) Primitive piles model [developed from (*85*)]. (**F**) Deep primitive layer (*86*).

Tackley 2000

Geochemistry, Seismology, Geodynamics

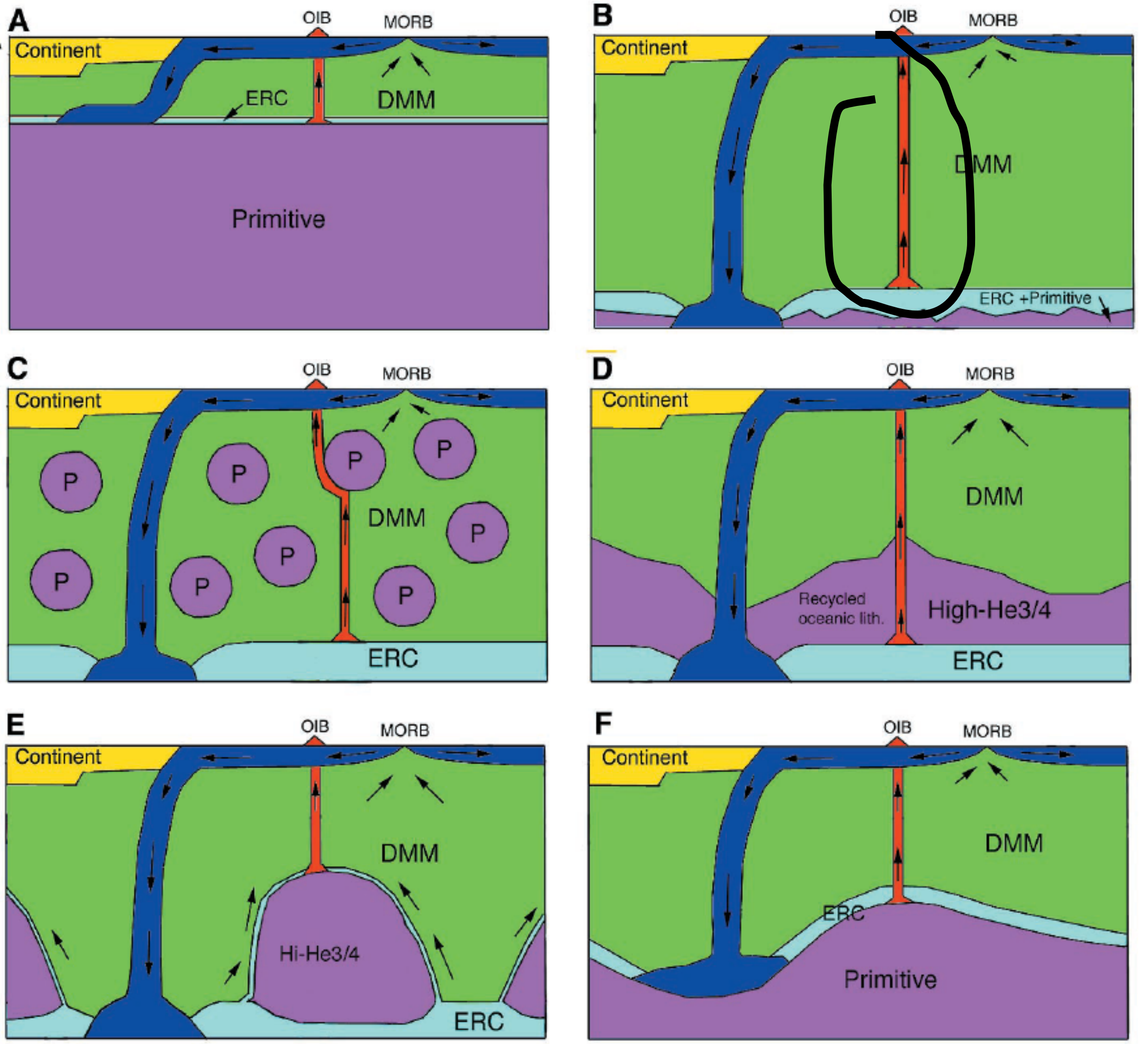

Fig. 2. Some possible locations of mantle reservoirs and relationship to mantle dynamics. Convective features: blue, oceanic plates/slabs; red, hot plumes. Geochemical reservoirs: dark green, DMM; purple, high $^3He/^4He$ ("primitive"); light green, enriched recycled crust (ERC). (**A**) Typical geochemical model layered at 660 km depth (*7*). (**B**) Typical geodynamical model: homogeneous except for some mixture of ERC and primitive material at the base. (**C**) Primitive blob model (*71*) with added ERC layer. (**D**) Complete recycling model (*83, 84*). (**E**) Primitive piles model [developed from (*85*)]. (**F**) Deep primitive layer (*86*).

Tackley 2000

Geochemistry, Seismology, Geodynamics

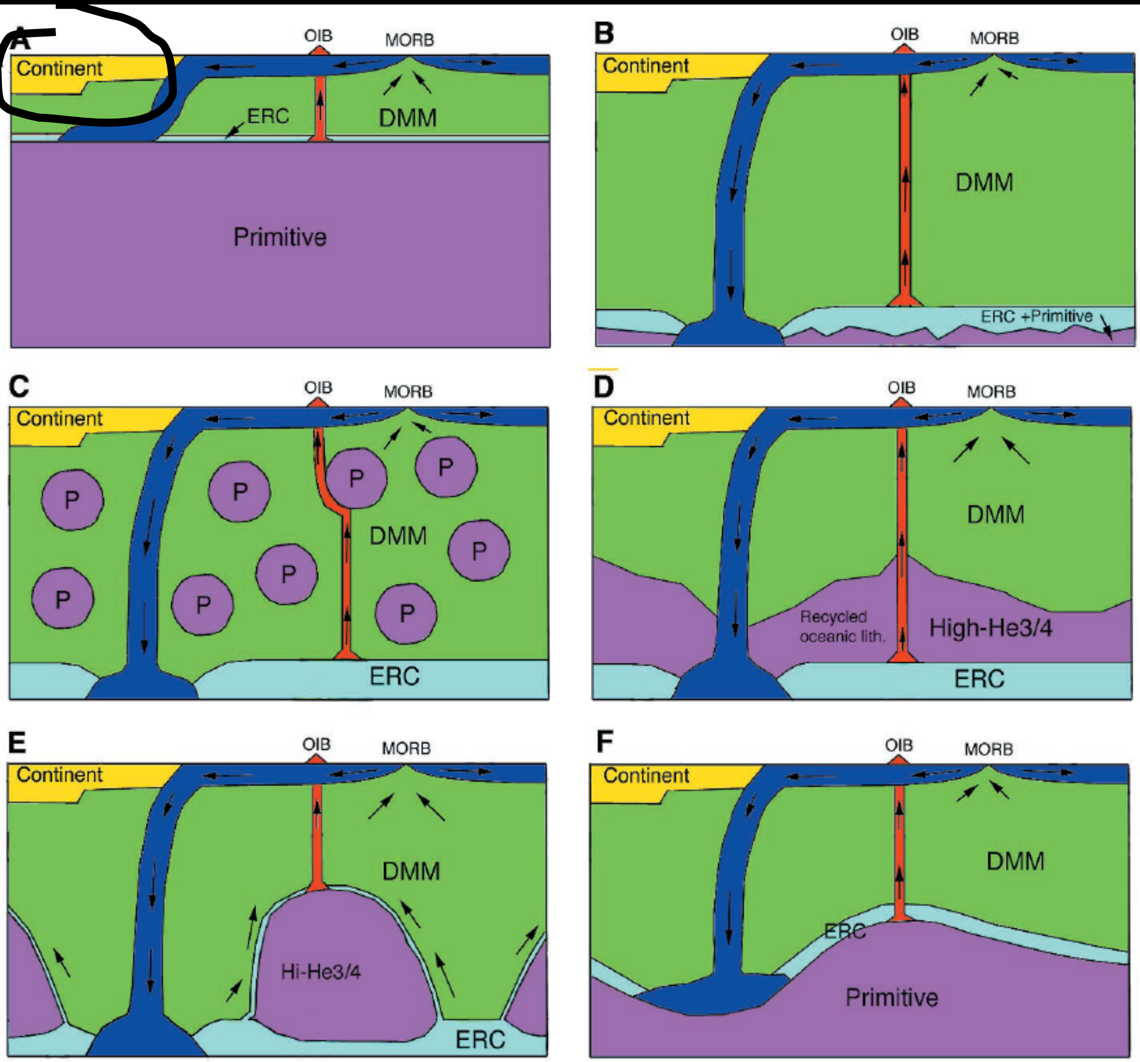

Fig. 2. Some possible locations of mantle reservoirs and relationship to mantle dynamics. Convective features: blue, oceanic plates/slabs; red, hot plumes. Geochemical reservoirs: dark green, DMM; purple, high $^3He/^4He$ ("primitive"); light green, enriched recycled crust (ERC). (**A**) Typical geochemical model layered at 660 km depth (*7*). (**B**) Typical geodynamical model: homogeneous except for some mixture of ERC and primitive material at the base. (**C**) Primitive blob model (*71*) with added ERC layer. (**D**) Complete recycling model (*83, 84*). (**E**) Primitive piles model [developed from (*85*)]. (**F**) Deep primitive layer (*86*).

Tackley 2000

Part 1: where do slabs go?

vertical mass transport in the mantle: role of the "670"

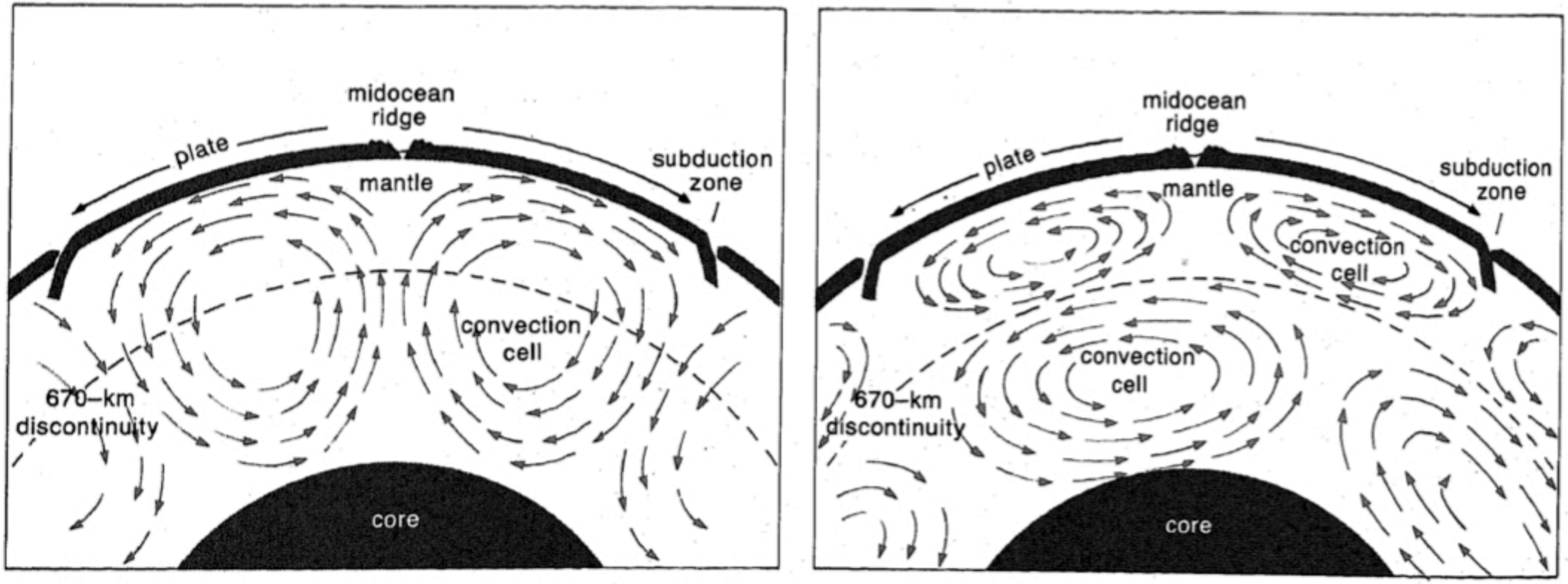

Figure 1. Many models of convection in the mantle, such as the two shown here in schematic cross section, have been proposed to account for the movement of the tectonic plates and for other features observed at the surface. Among the issues to be resolved is whether convective flow crosses between the upper and lower mantle at 670-km depth, where there is a sharp discontinuity in seismic velocities. Until very recently, the available data have been insufficient to resolve these issues; however, an expanded global network of seismographic stations now makes it possible to map details in the mantle.

484 American Scientist, Volume 72

Dziewonski and Anderson, 1984

slabs and the 660 discontinuity

Vol. 7, No. 4 April 1997

GSA TODAY

A Publication of the Geological Society of America

Global Seismic Tomography: A Snapshot of Convection in the Earth

Stephen P. Grand, *Department of Geological Sciences, University of Texas, Austin, TX 78712*
Rob D. van der Hilst, *Department of Earth and Planetary Sciences, Massachussetts Institute of Technology, Cambridge, MA 02139*
Sri Widiyantoro, *Research School of Earth Sciences, Australian National University, Canberra, ACT 0200, Australia*

ABSTRACT

Two new global high-resolution models of the P-wave and S-wave seismic structure of the mantle were derived independently using different inversion techniques and different data sets, but they show excellent correlation for many large-scale as well as smaller scale structures throughout the lower mantle. The two models show that high-velocity anomalies in the lower mantle are dominated by long linear features that can be associated with the sites of ancient subduction. The images suggest that most subduction-related mantle flow continues well into the lower mantle and that slabs may ultimately reach the core-mantle boundary. The models are available from anonymous ftp at maestro.geo.utexas.edu in directory pub/grand and at brolga.mit.edu in directory pub/GSAtoday.

INTRODUCTION

Since forming about 4.5 Ga, planet Earth has been cooling by means of relatively vigorous convection in its interior and by conductive heat loss across the cold thermal boundary layer at the top of the mantle (mainly the oceanic lithosphere). The primary force driving convection is the downward pull of gravity on the cold, dense lithosphere resulting in downwellings of slabs of subducted lithosphere. Understanding the nature of the

Tomography *continued on p. 2*

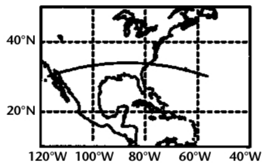

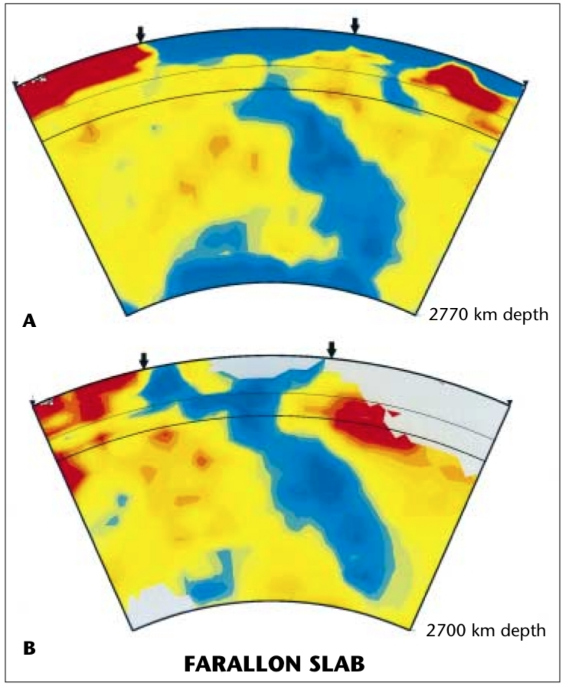

Figure 1. Cross sections of mantle P-wave (A) and S-wave (B) velocity variations along a section through the southern United States. The endpoints of the section are 30.1°N, 117.1°W and 30.2°N, 56.4°W. The images show variations in seismic velocity relative to the global mean at depths from the surface to the core-mantle boundary. Blues indicate faster than average and reds slower than average seismic velocity. The large tabular blue anomaly that crosses the entire lower mantle is probably the descending Farallon plate that subducted over the past ~100 m.y. Differences in structure between the two models in the transition zone (400 to 660 km depth) and at the base of the mantle are probably due to different data sampling in the two studies.

Grand and van der Hilst (mid 1990s)

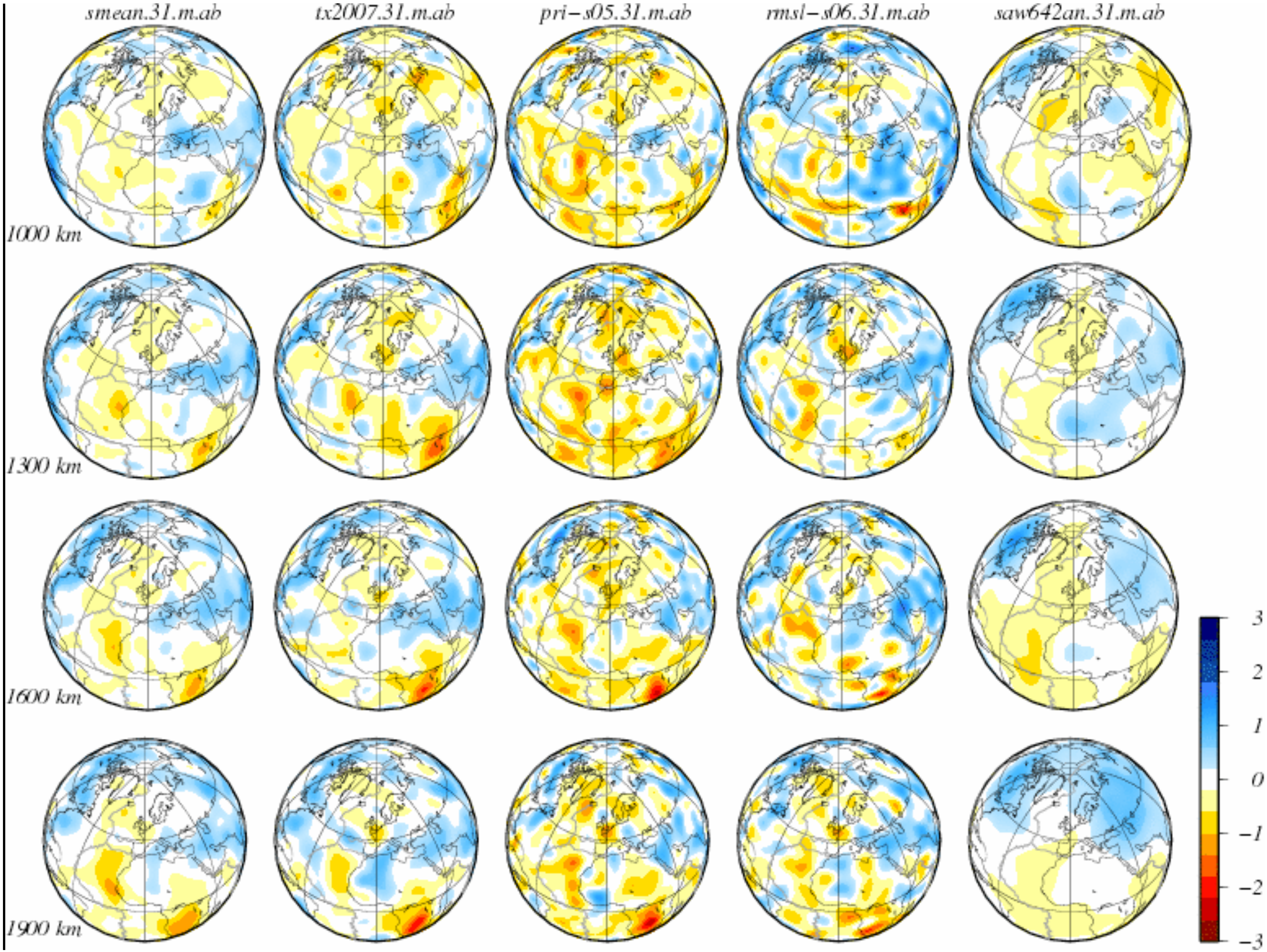

smean.31.m.ab
tx2007.31.m.ab
pri−s05.31.m.ab
rmsl−s06.31.m.ab
saw642an.31.m.ab
1000 km
1300 km
1600 km
1900 km
3
2
1
0
−1
−2
−3

sinking and floating slabs

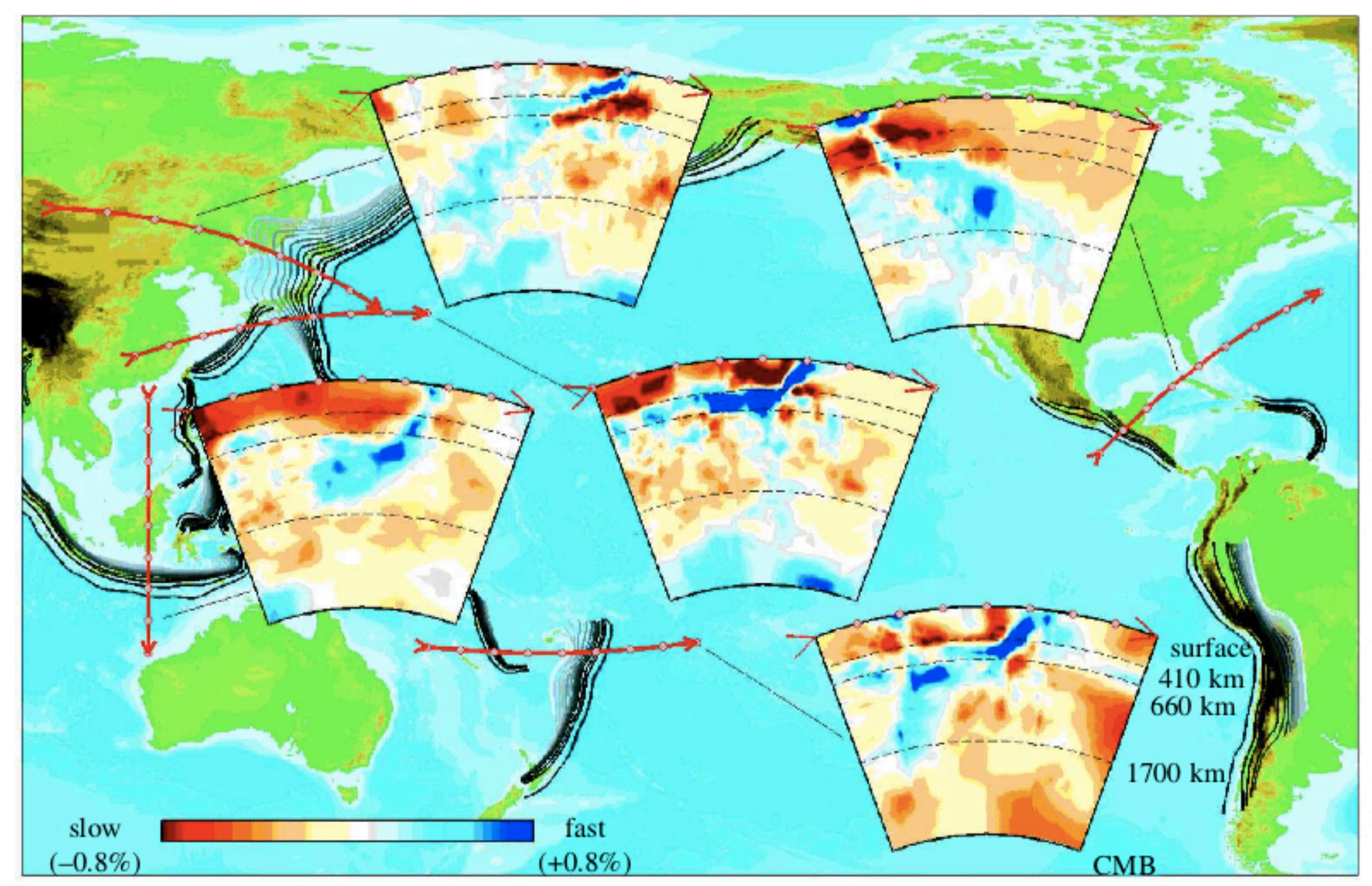

Albarède and van der Hilst, 2002

deep slabs: mapped by tomography and predicted by geodynamics

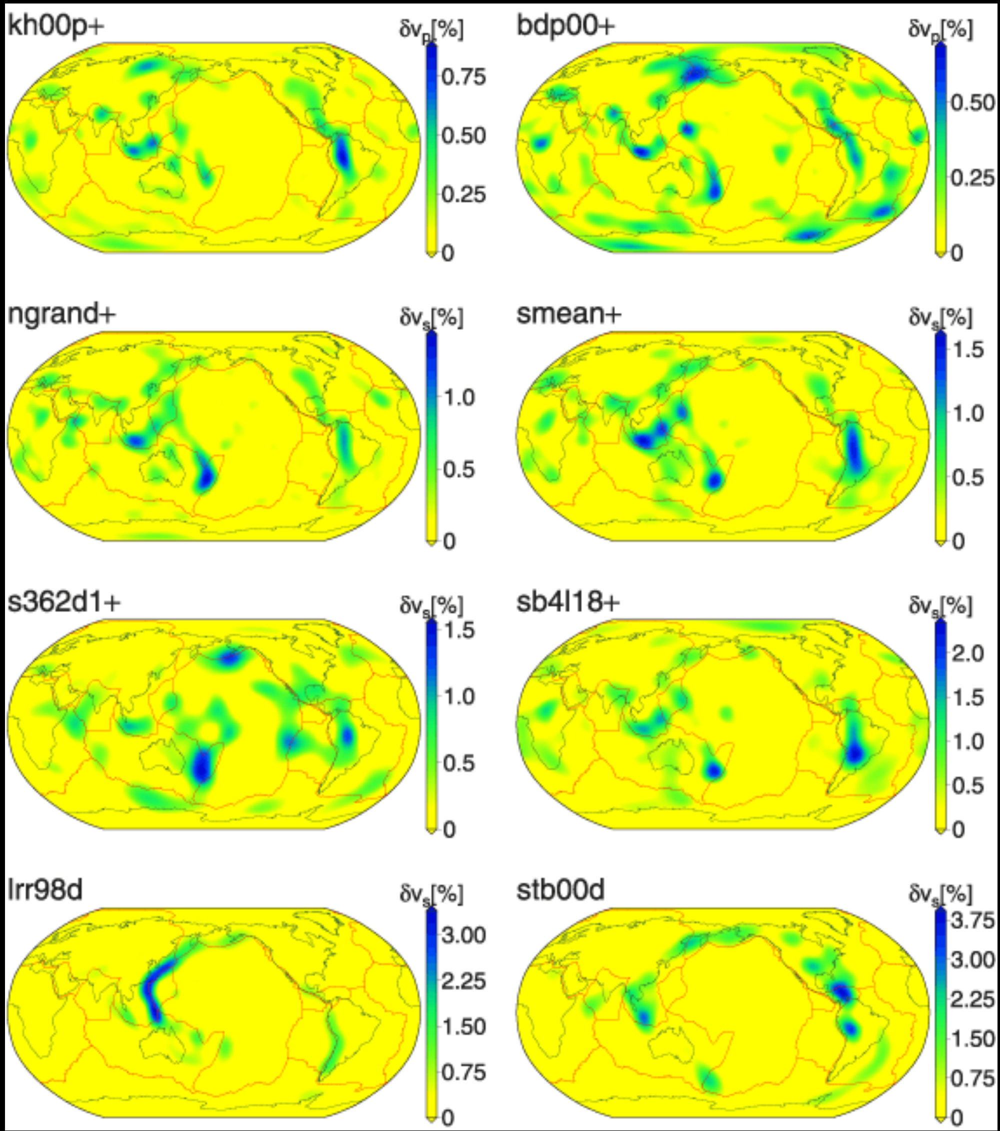

tomography (>0 only) and geodynamics slab models at 850 km

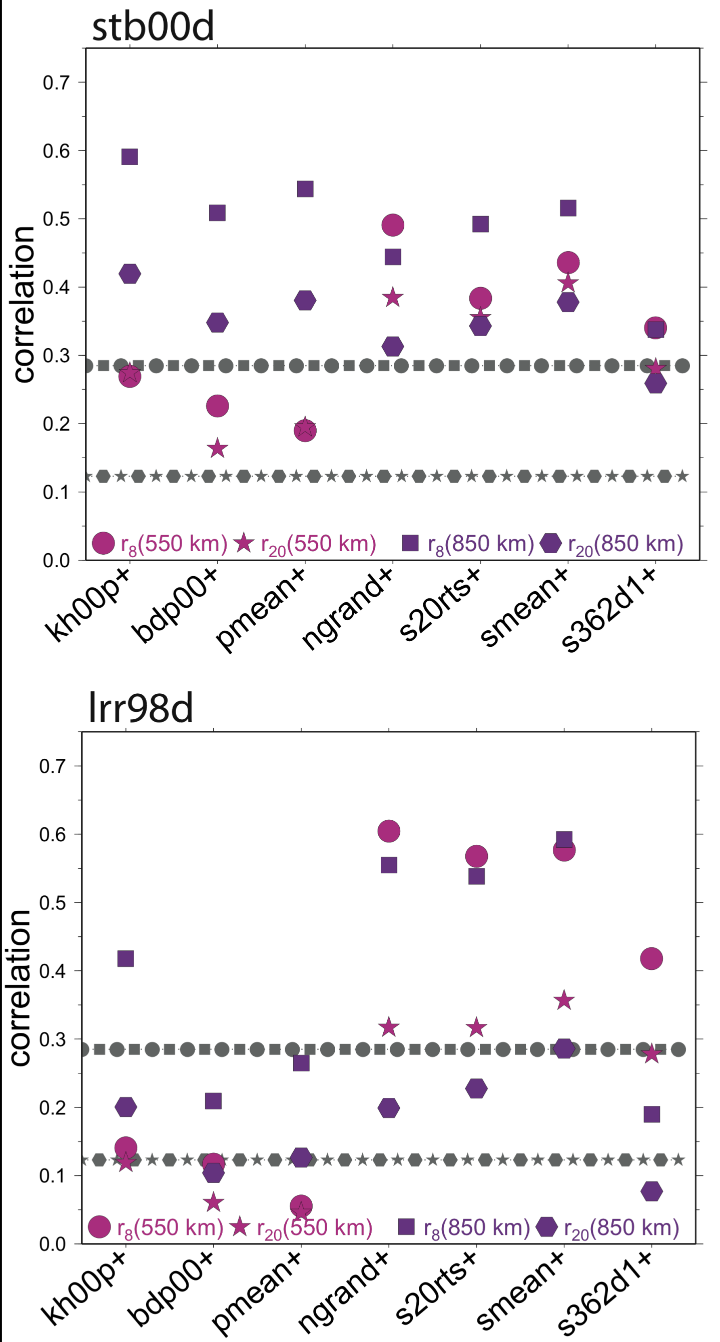

Becker and Boschi, 2002

S tomography

ratio of harmonic spectra: positive vs. negative anomalies (smean)

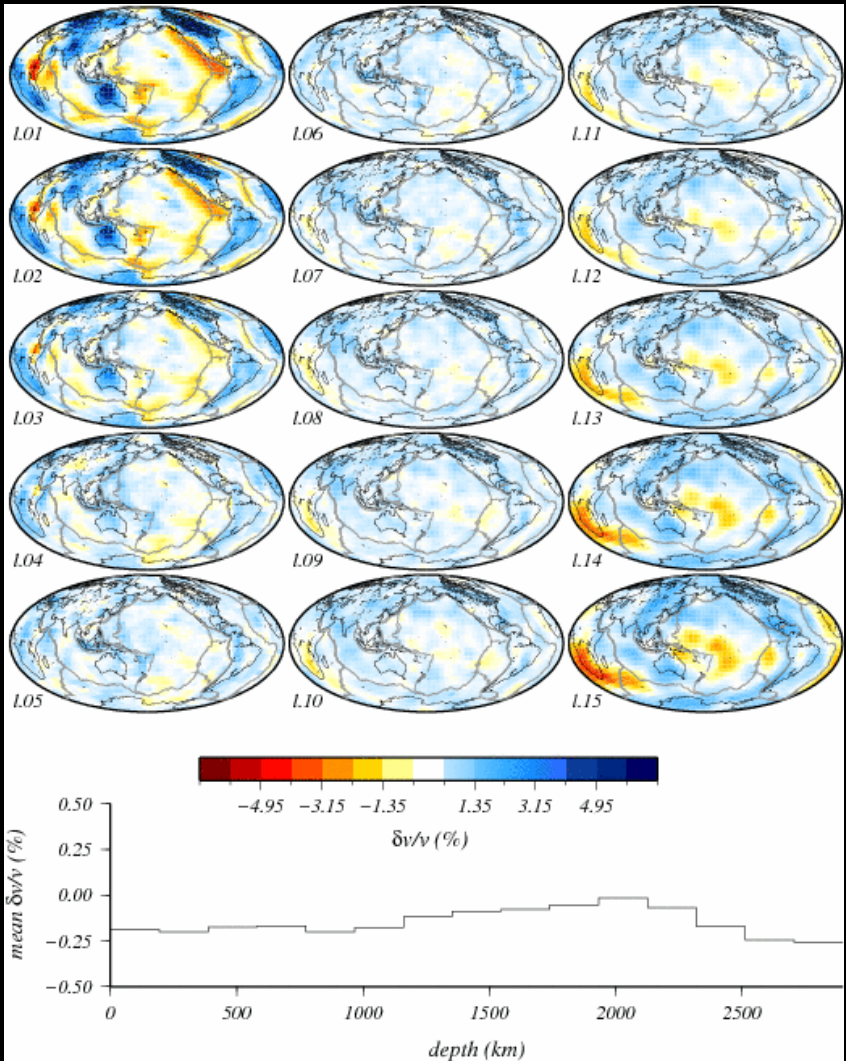

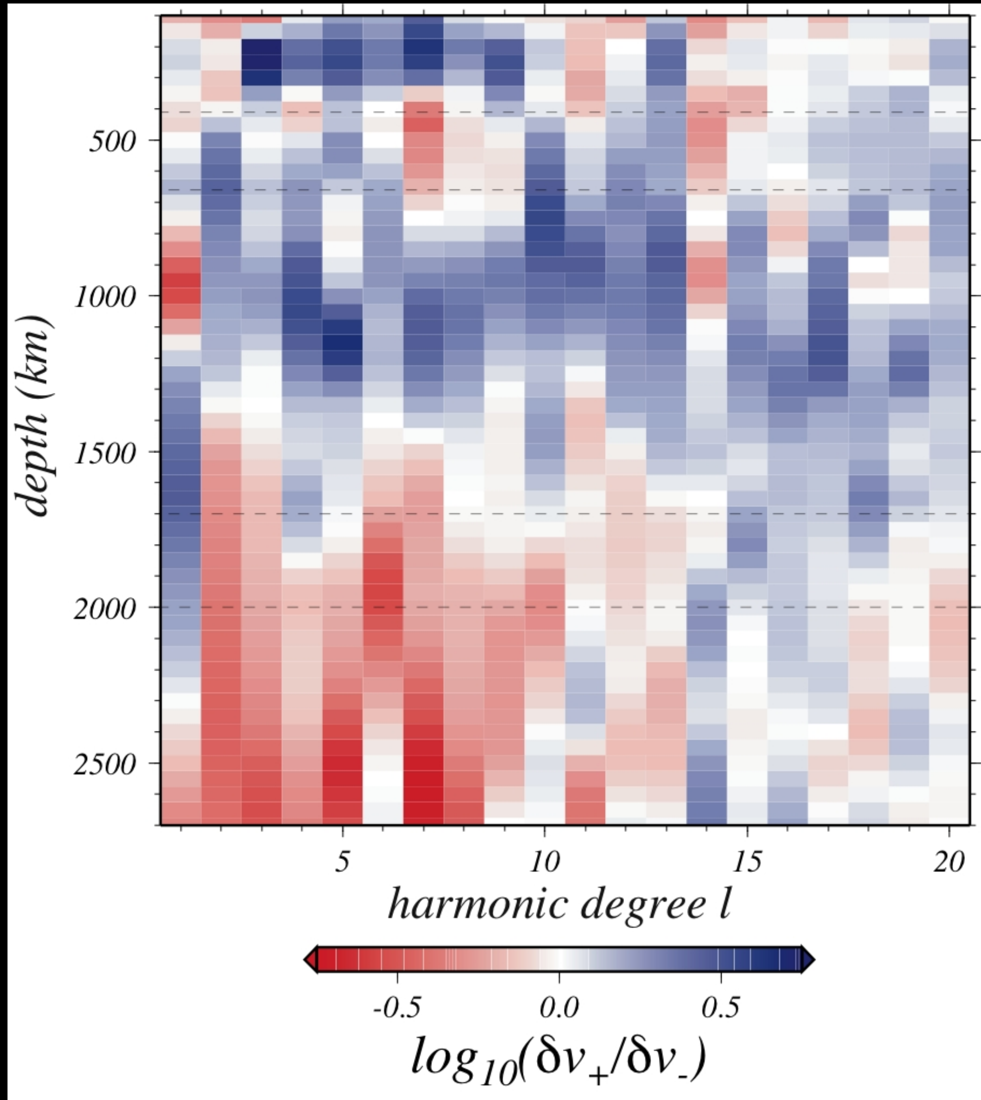

Boschi, Becker and Steinberger, 2007

deep viscosity "hill"

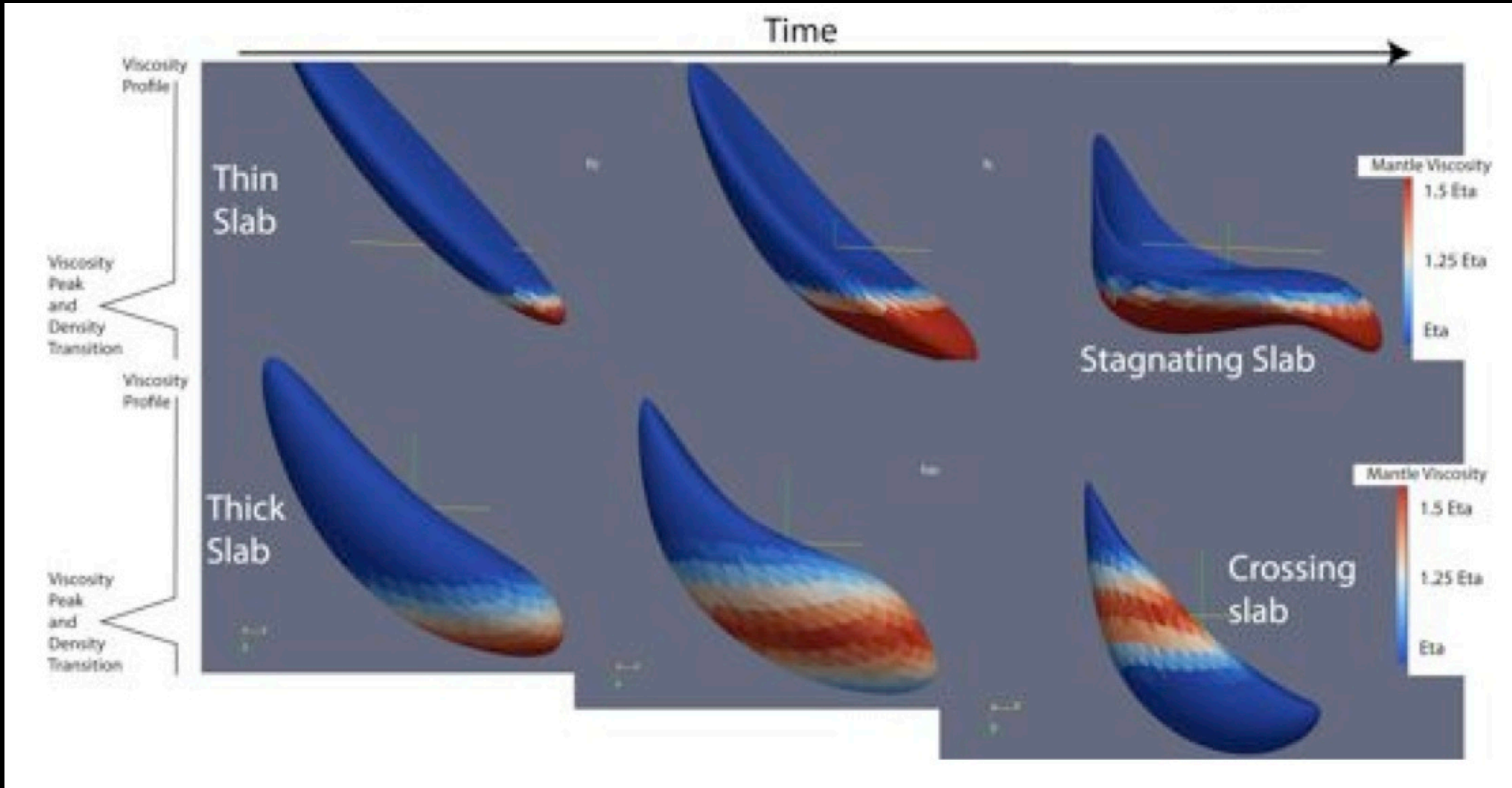

Morra, Yuen, Boschi. Chatelain, Koumoutsakos, Tackley, 2009

“670” as a thermal boundary layer

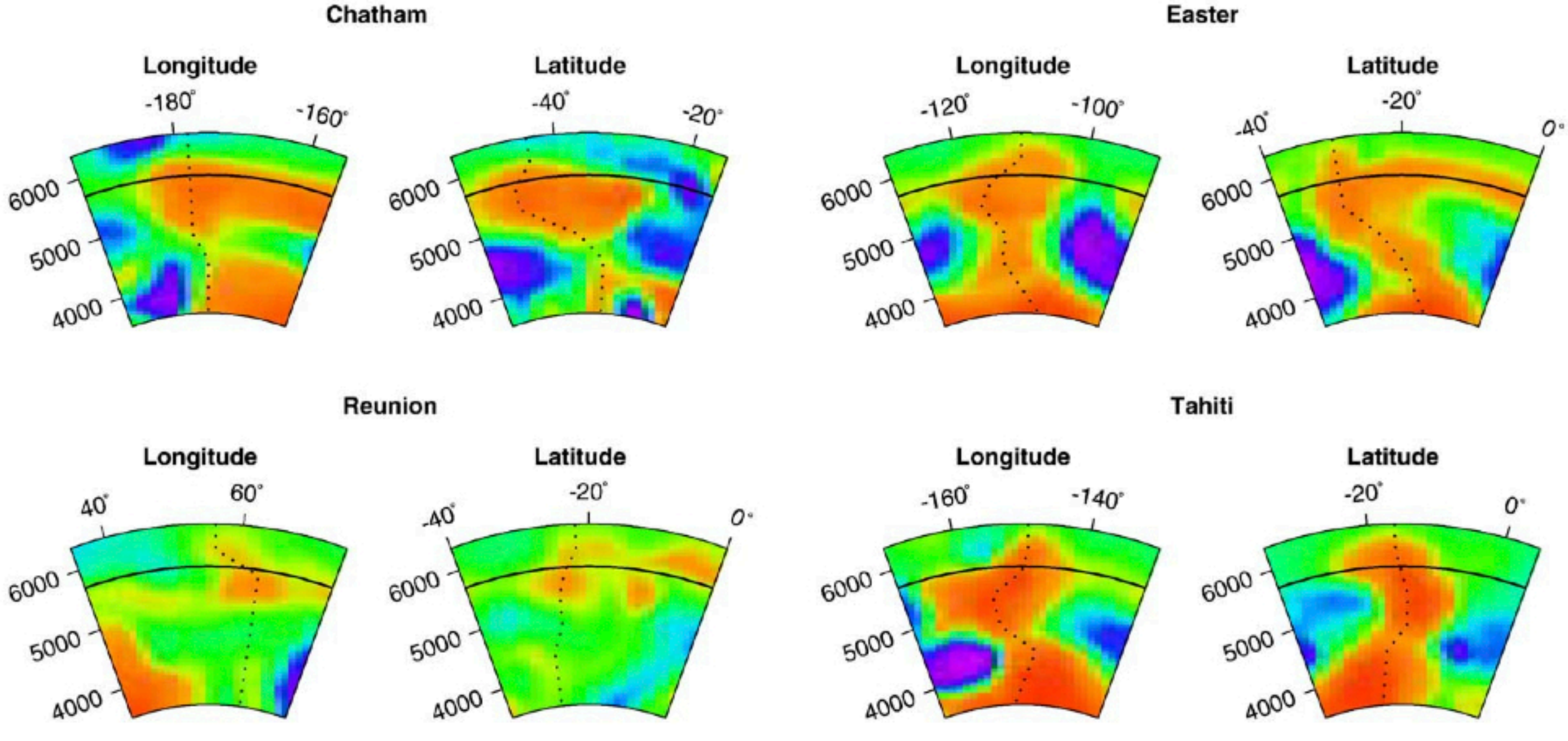

Fig. 2. Four examples of plumes that widen or even get stuck below the 670 km discontinuity. Resolution tests similar to the one shown in Fig. 1 show that the broadening or deflection at the top of the mantle is resolved for each of these plumes. The temperature scale is the same as in Fig. 1 (top).

Nolet, Karato and Montelli, 2006

Part 2: the origin of hotspots

(work by Boschi, Becker and Steinberger 2007, 2008, plus some new results by Thorsten Becker)

Plumes as the origin of hotspots (Wilson 1971)

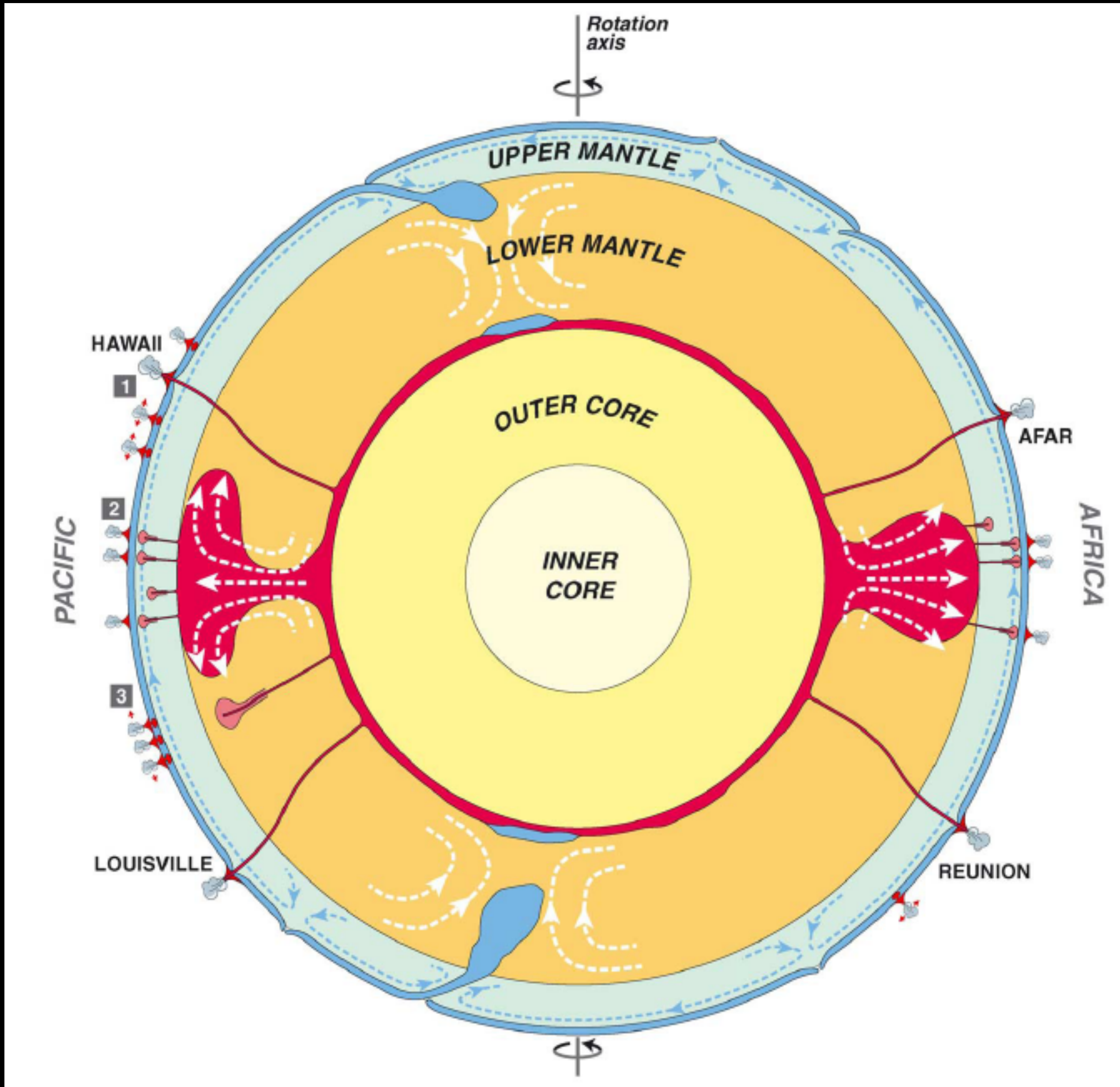

Courtillot et al. 2003

Plume clusters

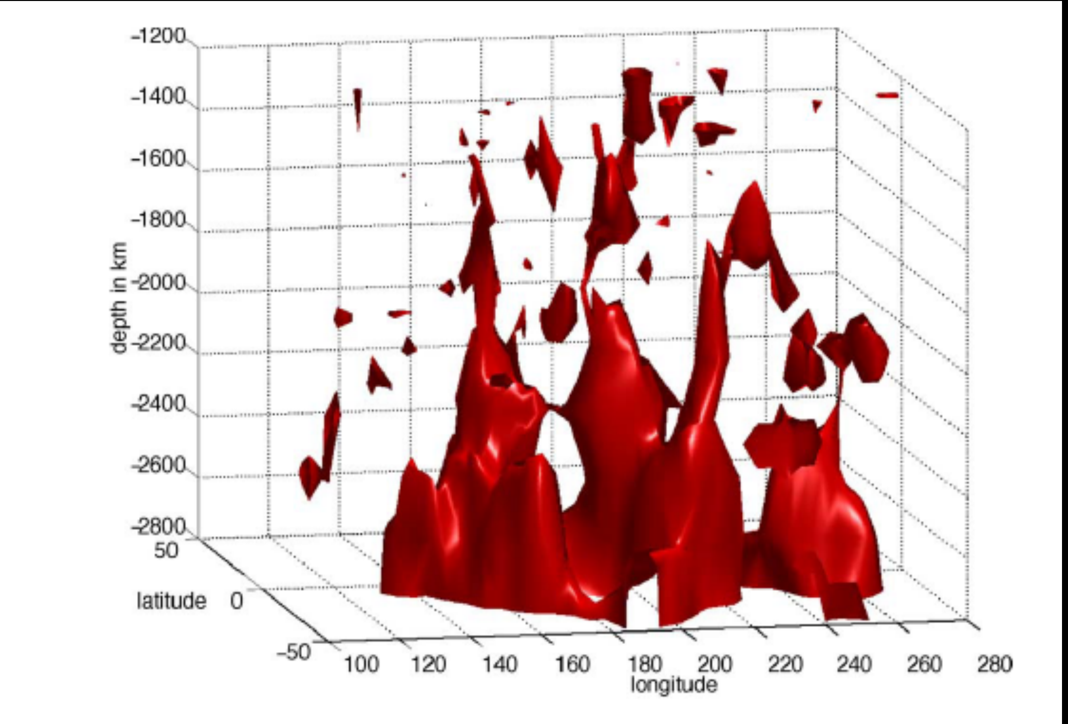

Fig. 3. Isovelocity surfaces (encompassing negative perturbations of 1.1% or more) of the Pacific superplume.

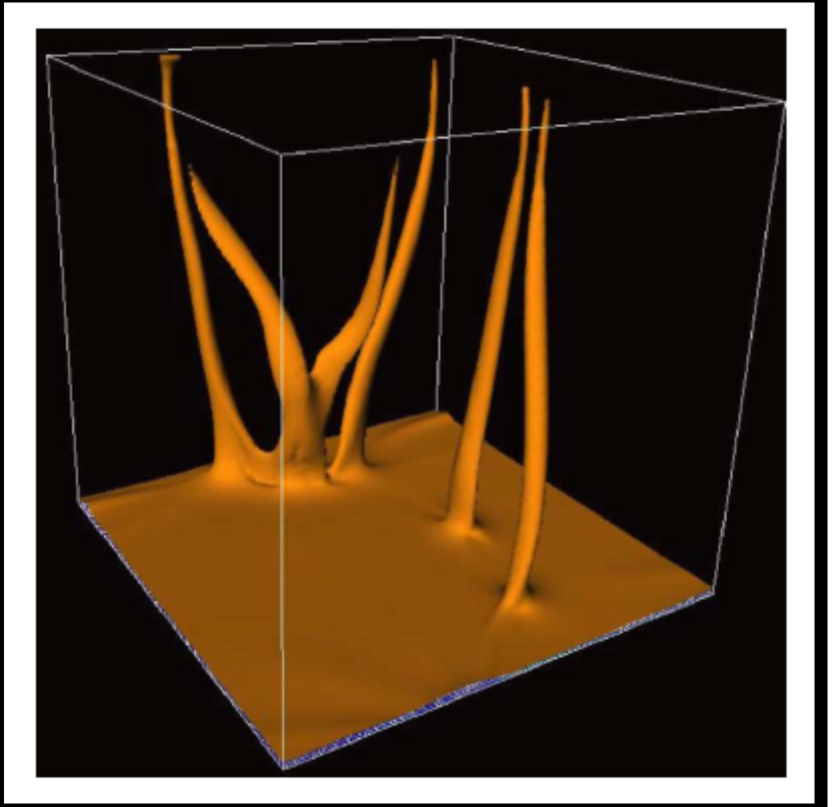

Schubert et al. 2004

Hotspot catalogue: dynamic models of corresponding plumes

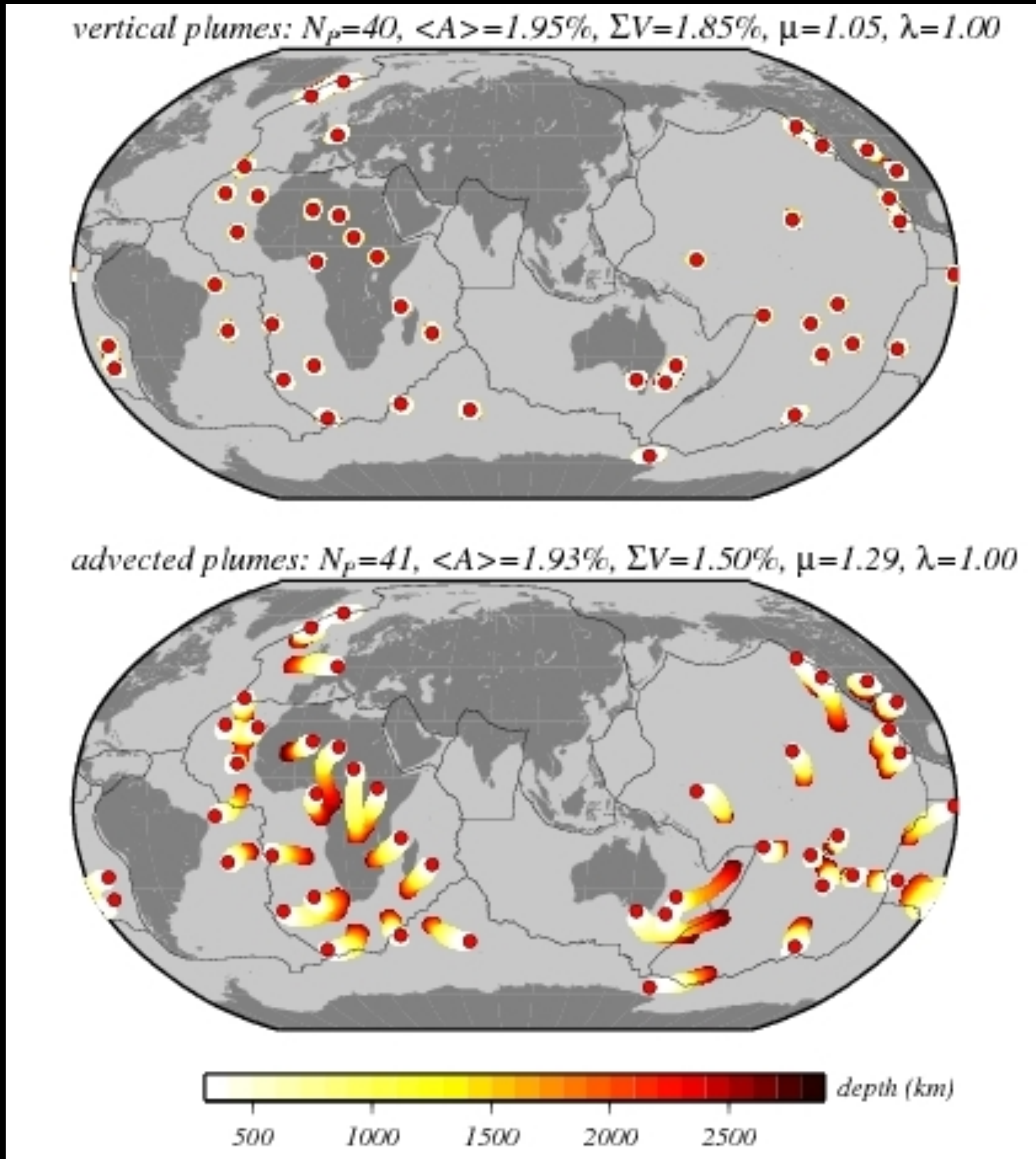

Resolving power of tomography

Plume model input

input @ 500 km

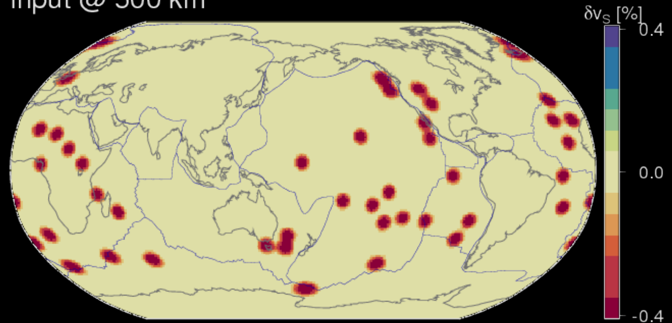

input @ 1500 km

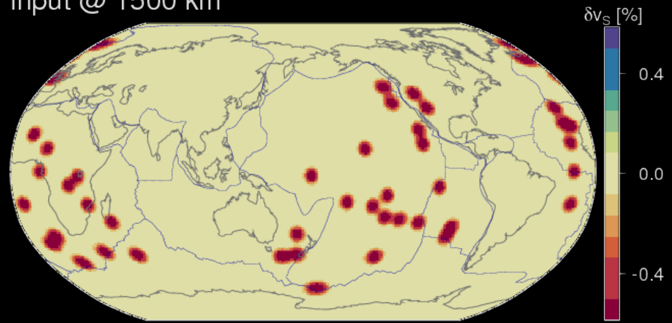

input @ 2500 km

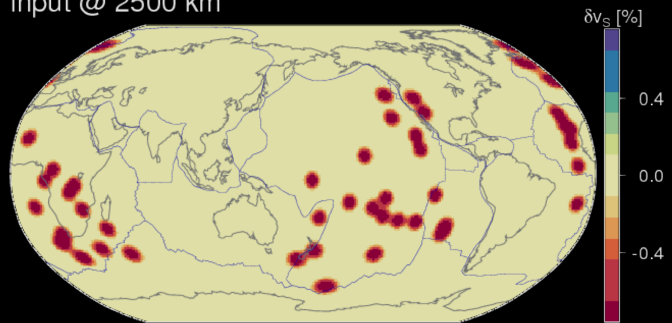

depth

Inversion output

synthetics

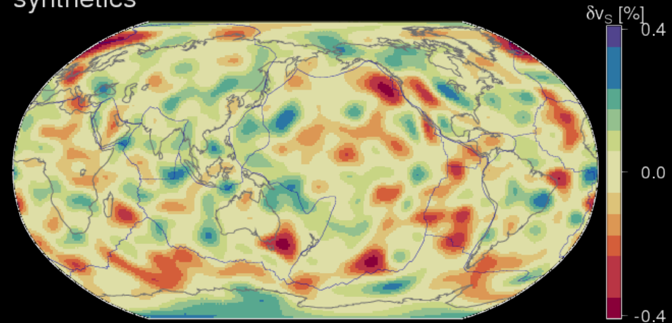

synthetics

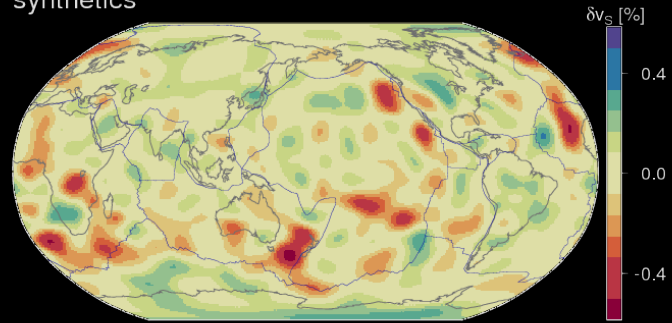

synthetics

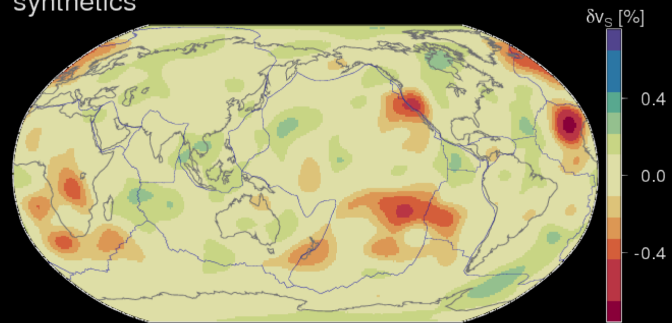

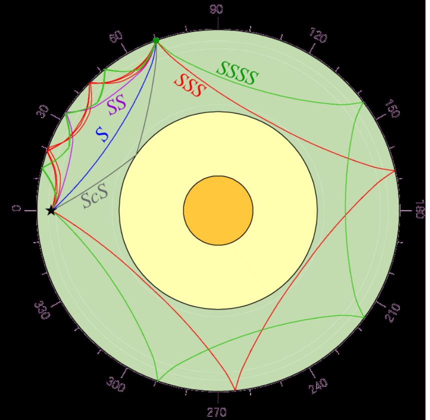

S body-wave data from Simmons and Grand. Noise added before inversion.

S tomographic models; 12 likely deep plumes; advection vs. no advection

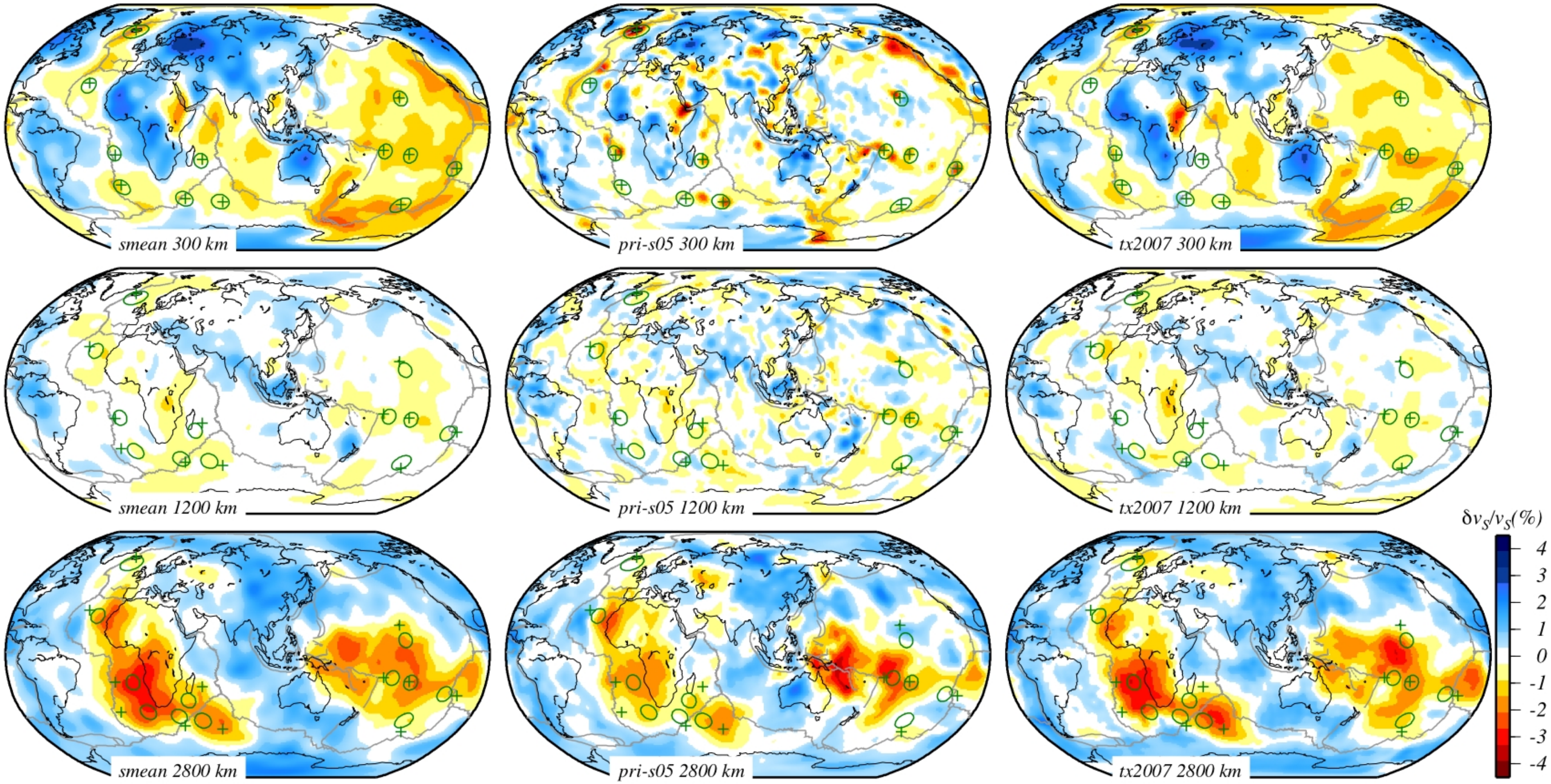

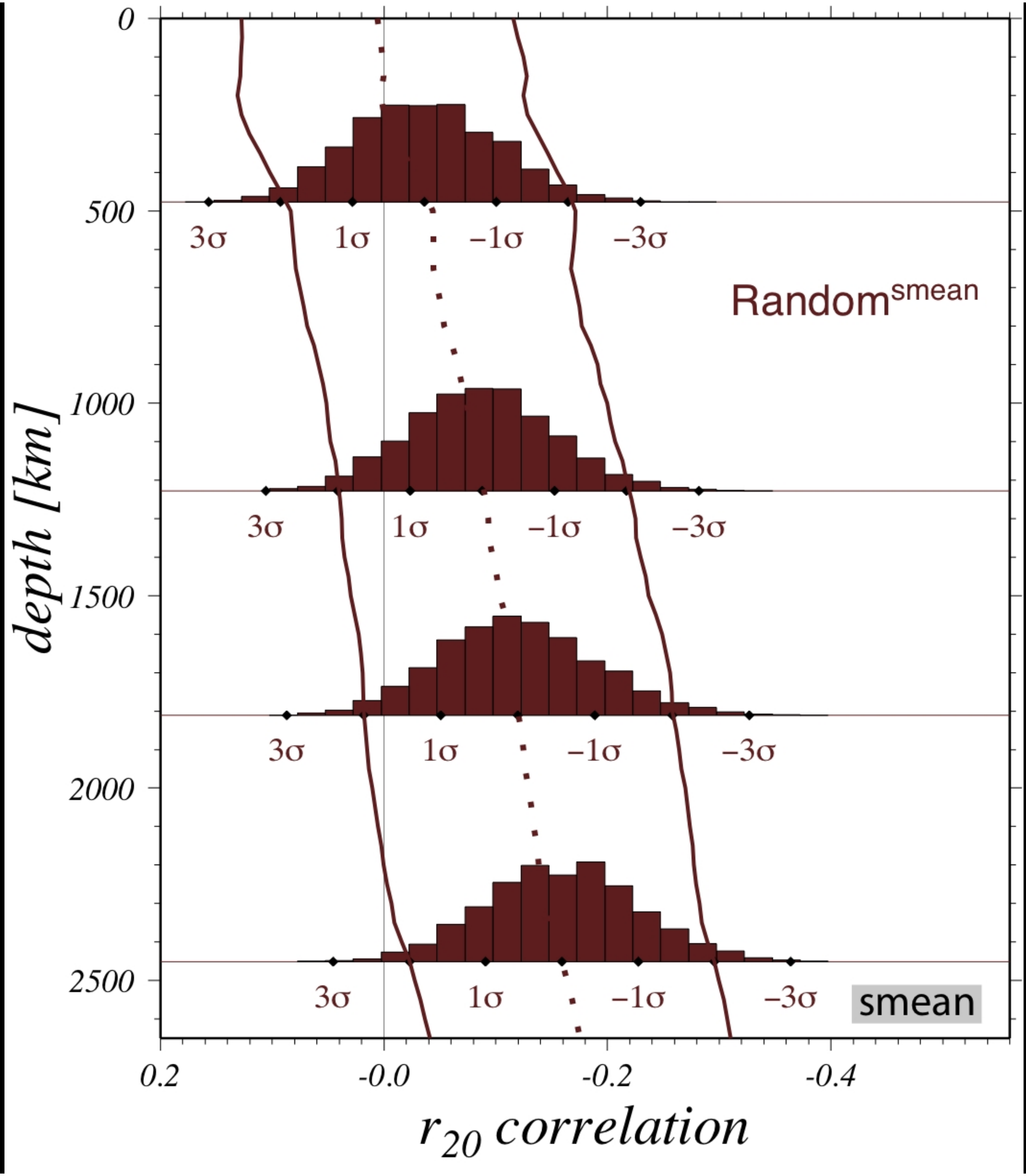

Random^{smean}
smean
3σ
1σ
−1σ
−3σ
0
500
1000
1500
2000
2500
0.2
-0.0
-0.2
-0.4
depth [km]
r_{20} correlation

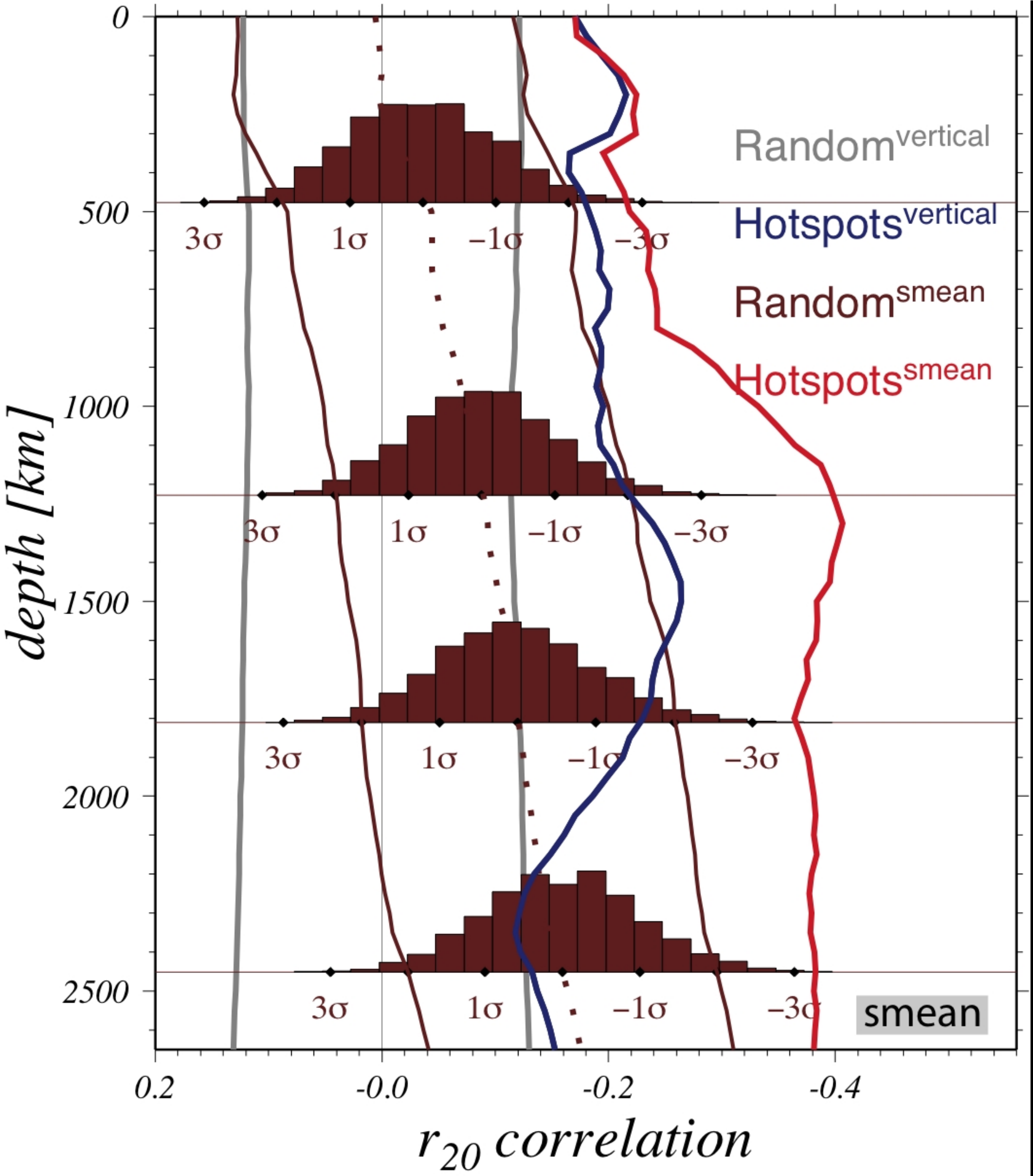

0
500
1000
1500
2000
2500
depth [km]
3σ
1σ
−1σ
−3σ
Random^{vertical}
Hotspots^{vertical}
Random^{smean}
Hotspots^{smean}
smean
0.2
-0.0
-0.2
-0.4
r_{20} correlation

Significance of correlation evaluated with a Montecarlo approach

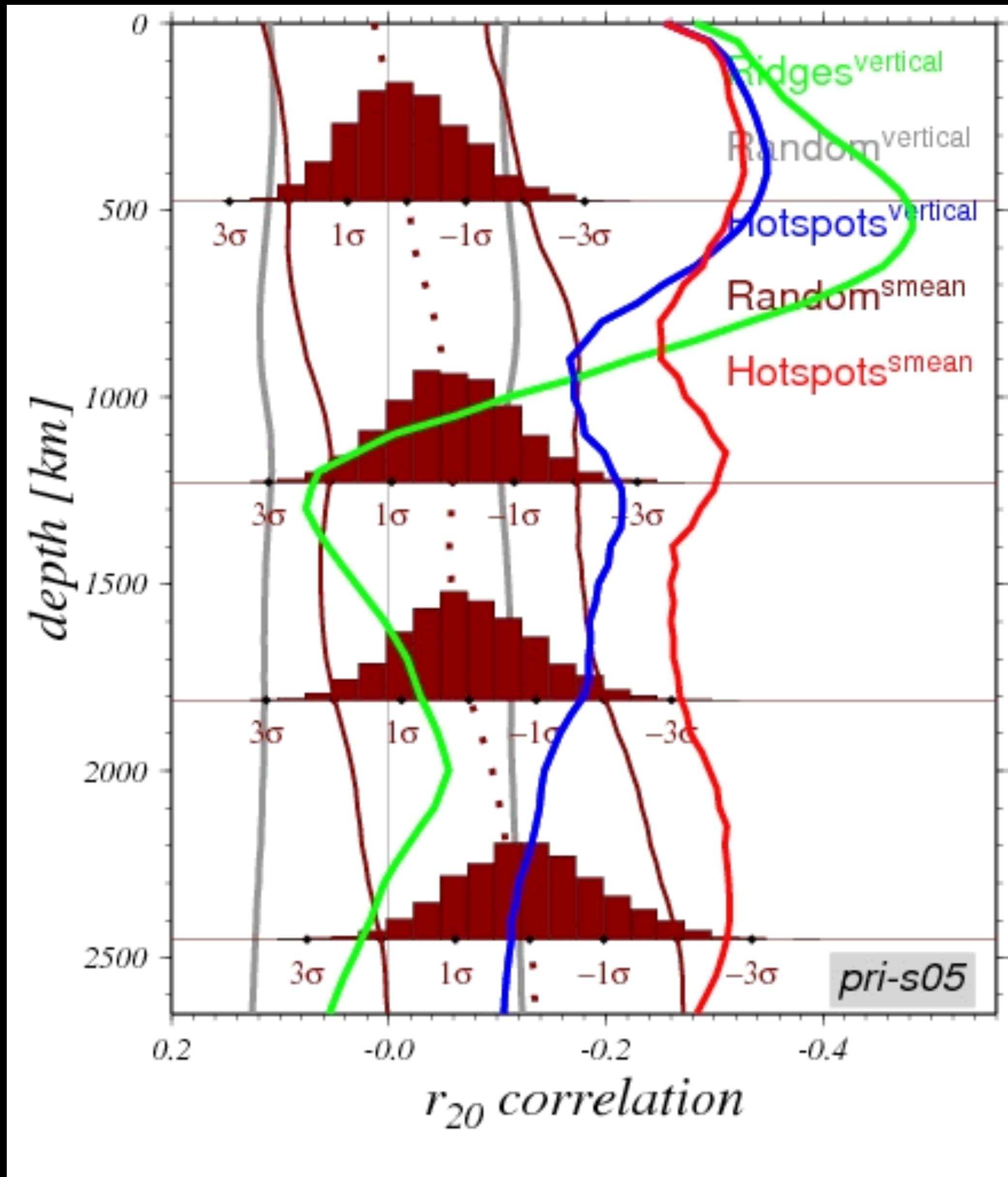

S

Significance of correlation evaluated with a Montecarlo approach

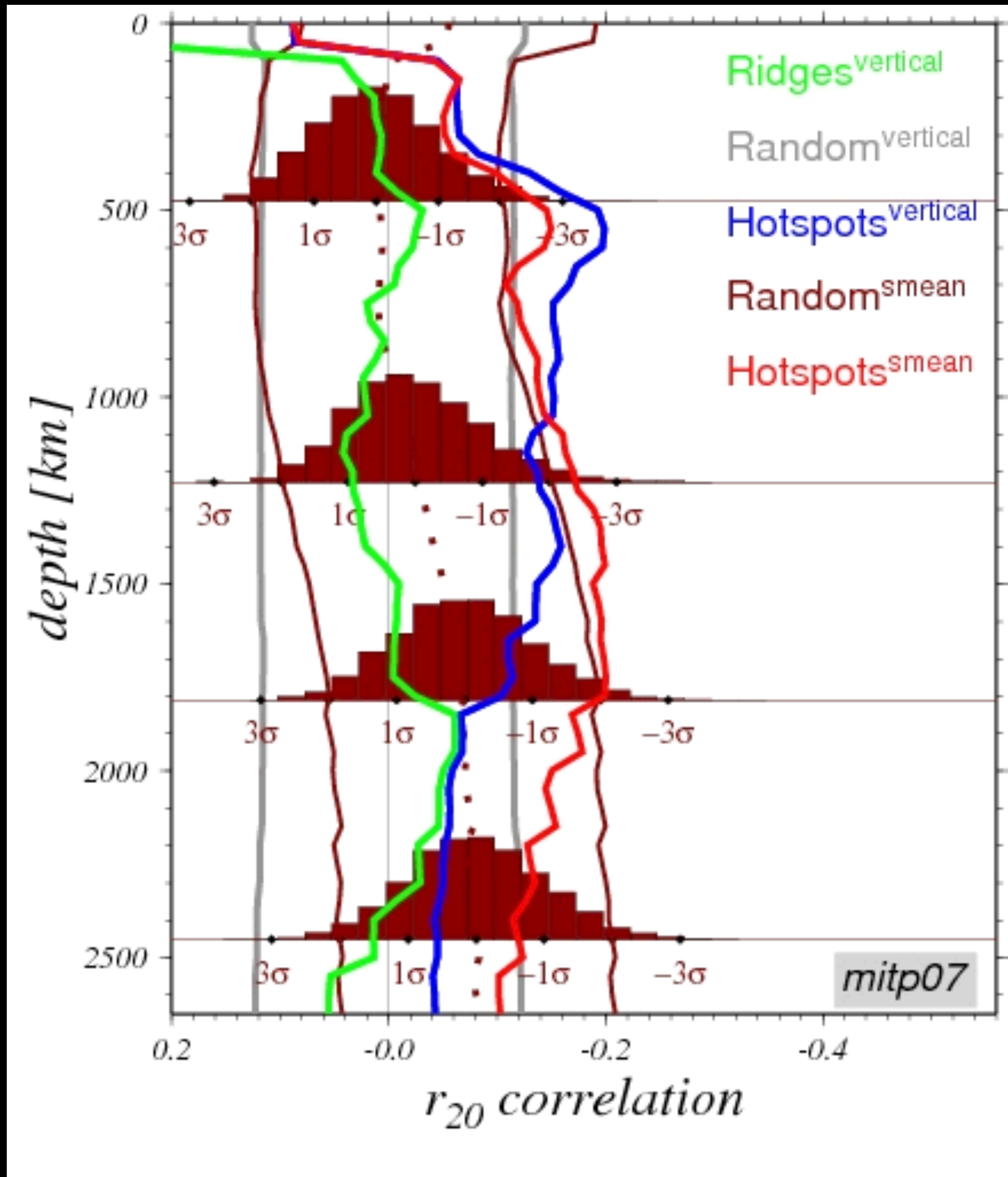

P

we use values of seismic anomalies within dynamically modeled plumes to evaluate which tomography-imaged plumes are likely to be real

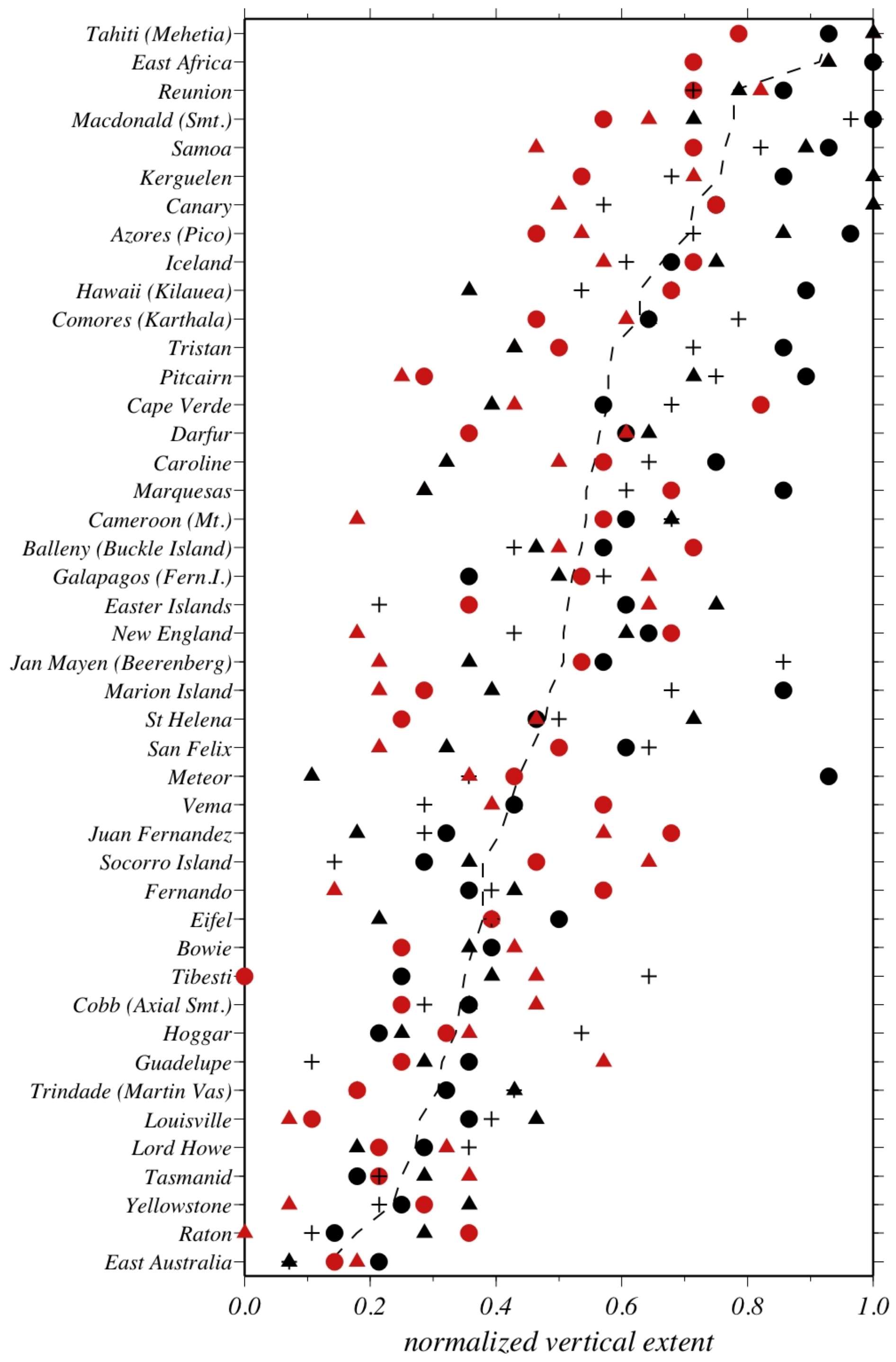

where are the hotspots likely to form from deep plumes?

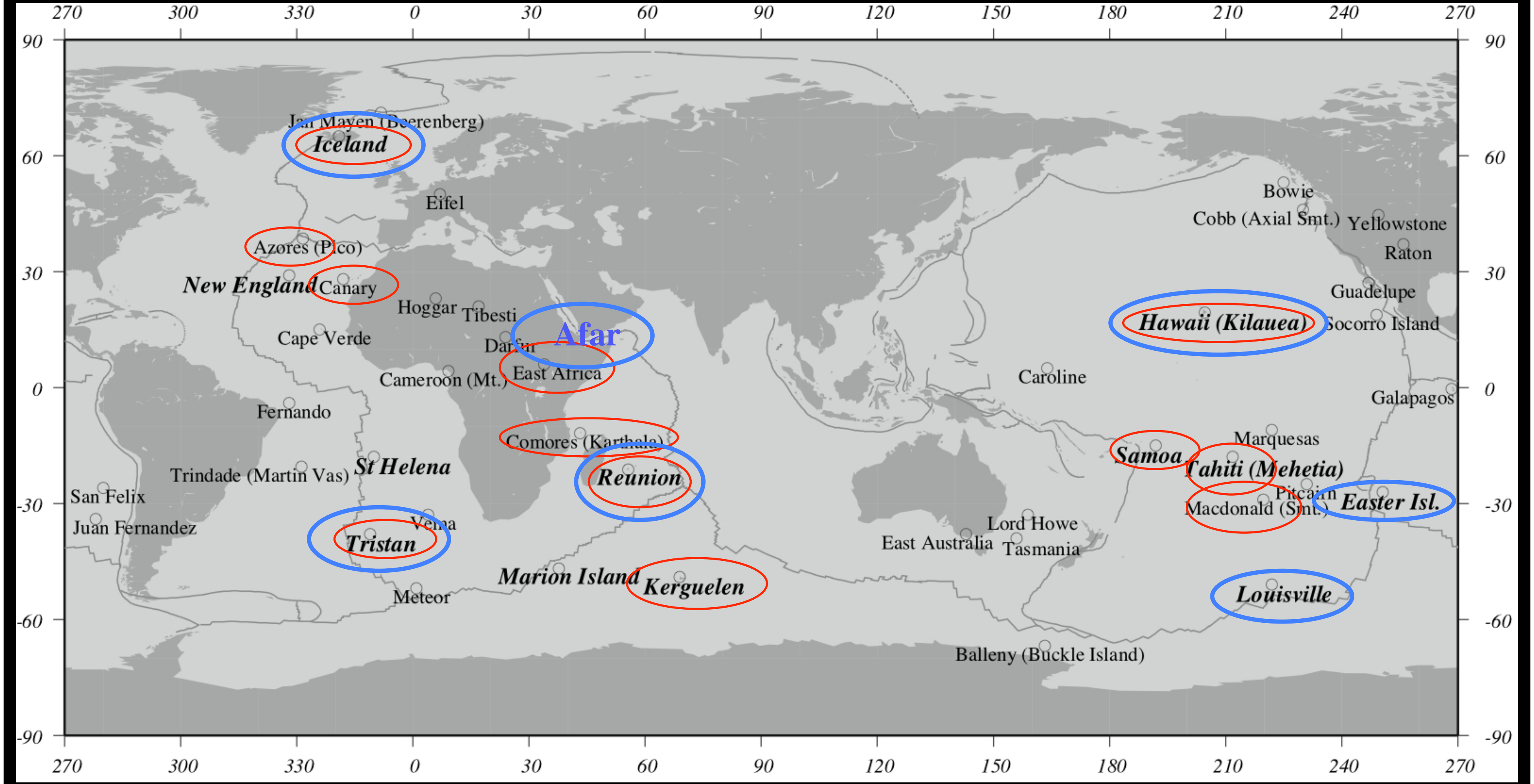

Courtillot et al. 2003

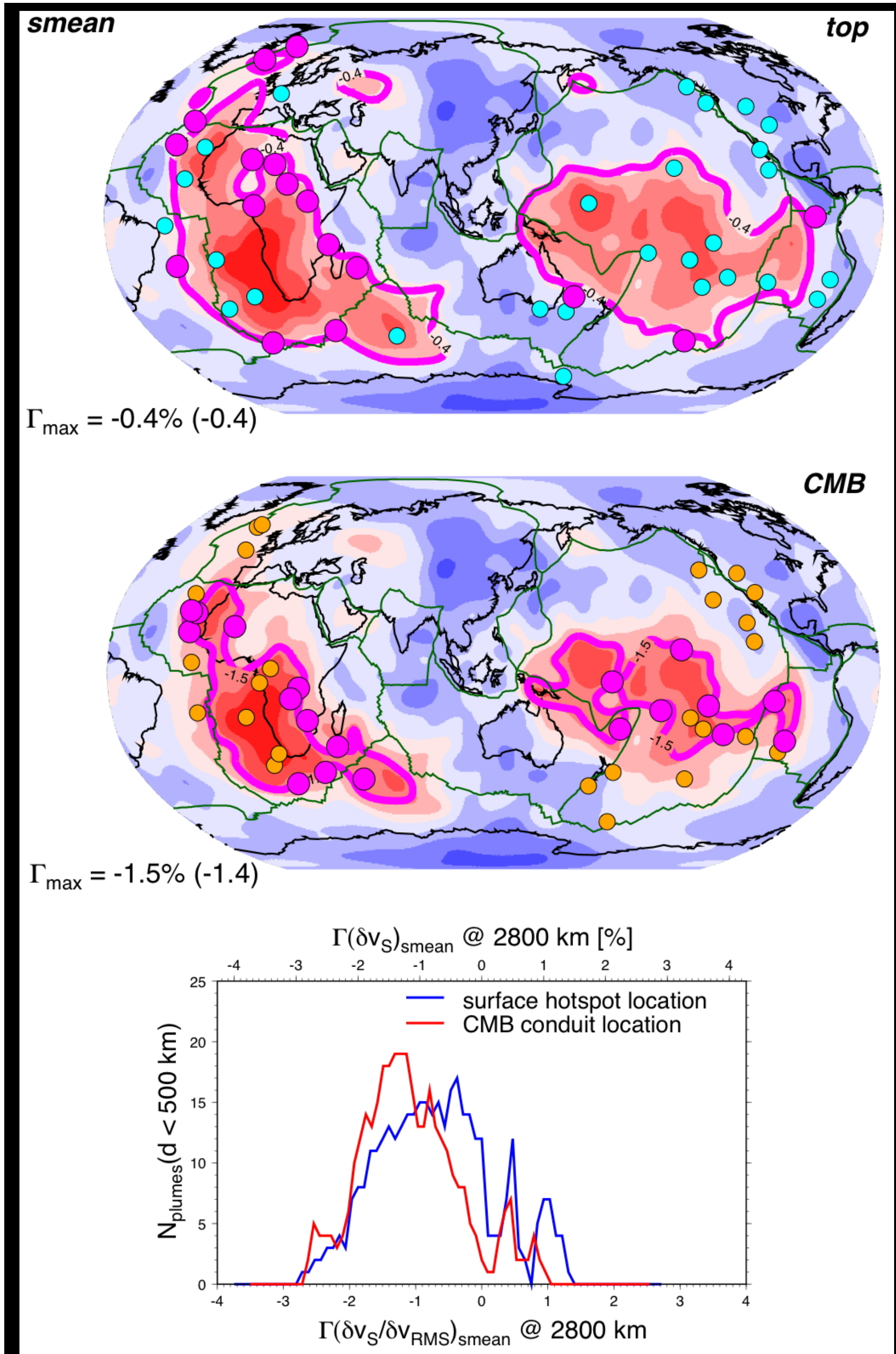

plume source location

Hotspot locations (circles), lowermost mantle tomography. A “contour” (purple line) of LLSVPs is identified that maximizes the number of nearby hotspots (purple circles)

Same, but hotspot locations are replaced by the locations of advected plume sources: LLSVP-contour collapses towards center of LLSVP itself

Number of hotspots vs. value on LLSVP-contour

Part 3: upper mantle and transition zone

S tomography (body waves)

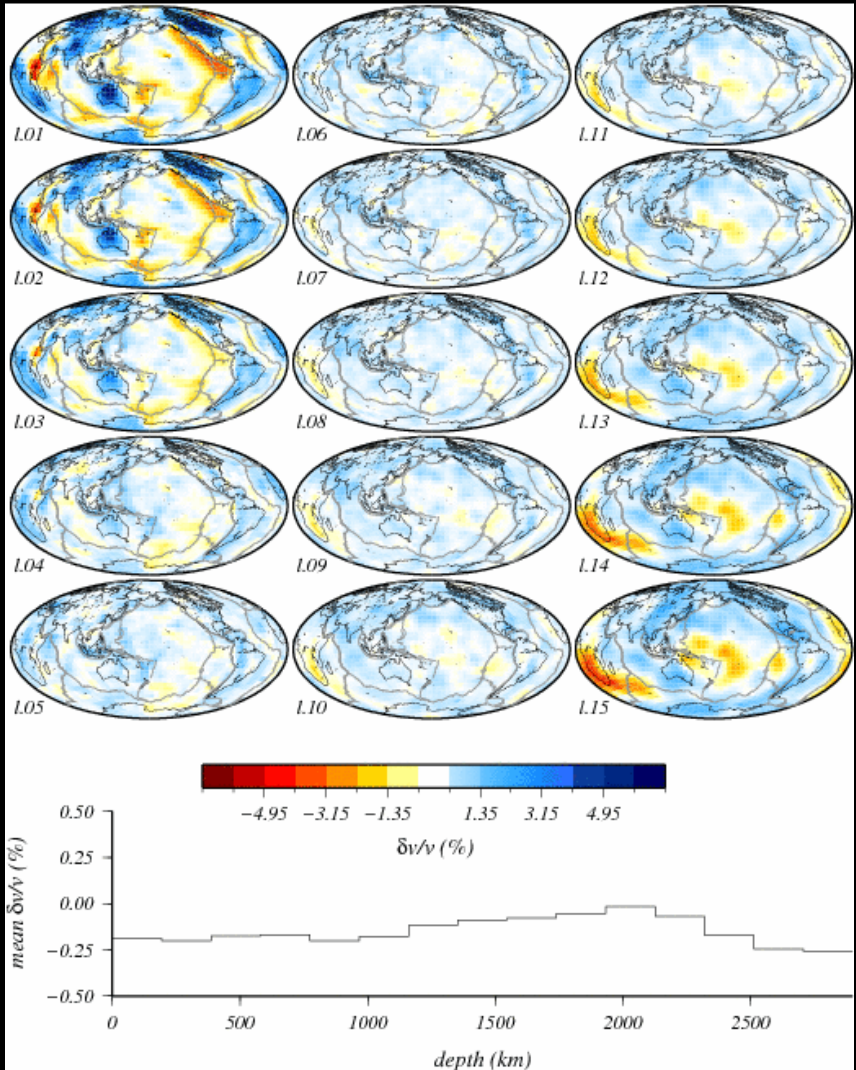

where should we put a discontinuity?

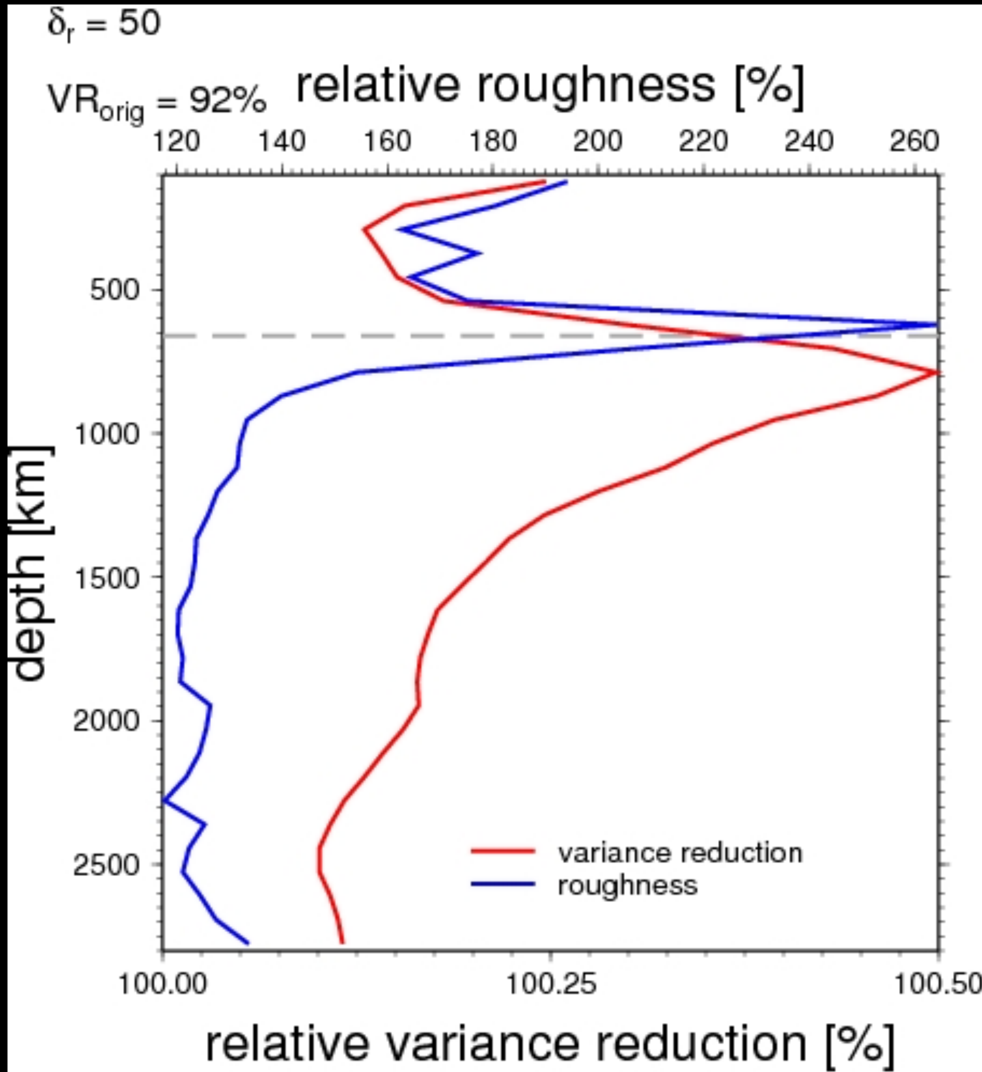

Becker and Boschi, 2009

surface-wave tomography

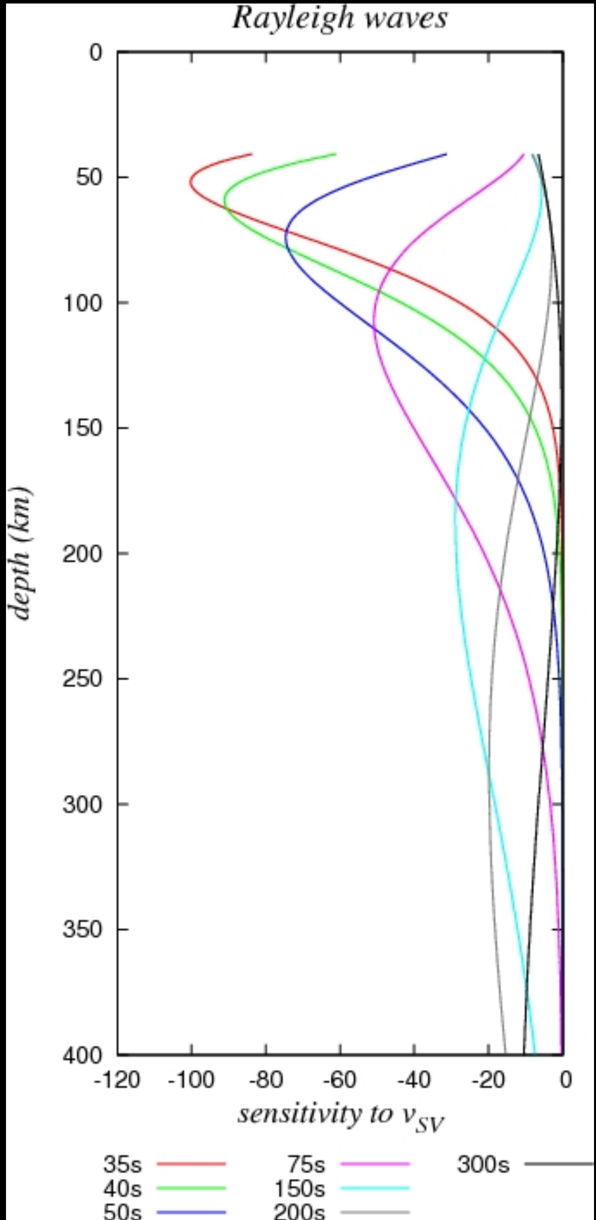

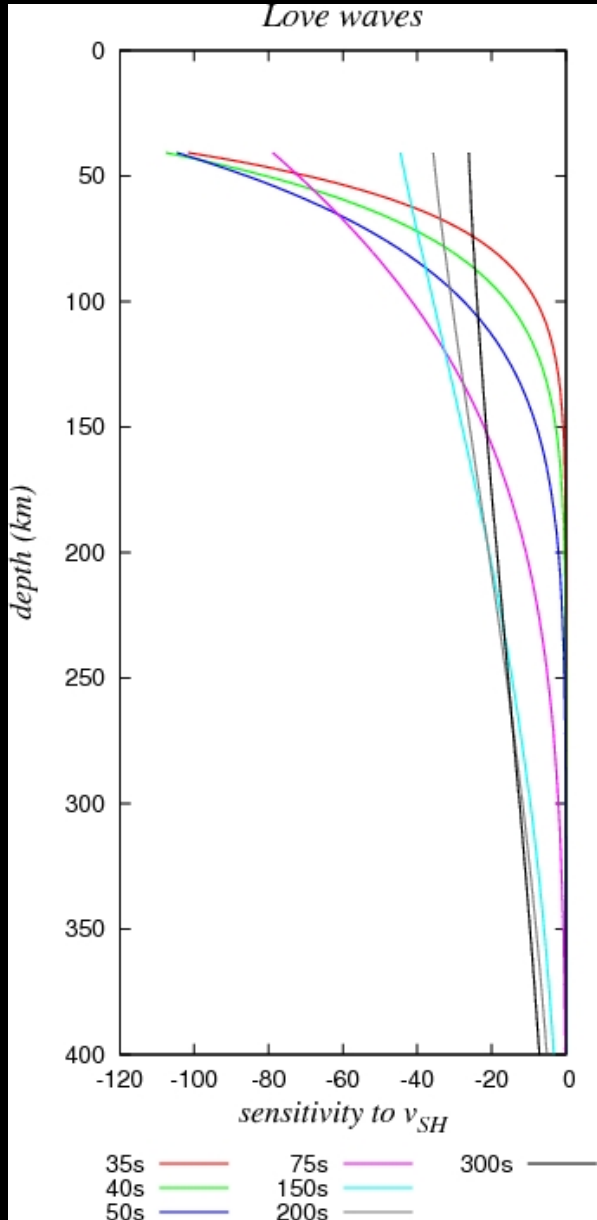

improvement in database

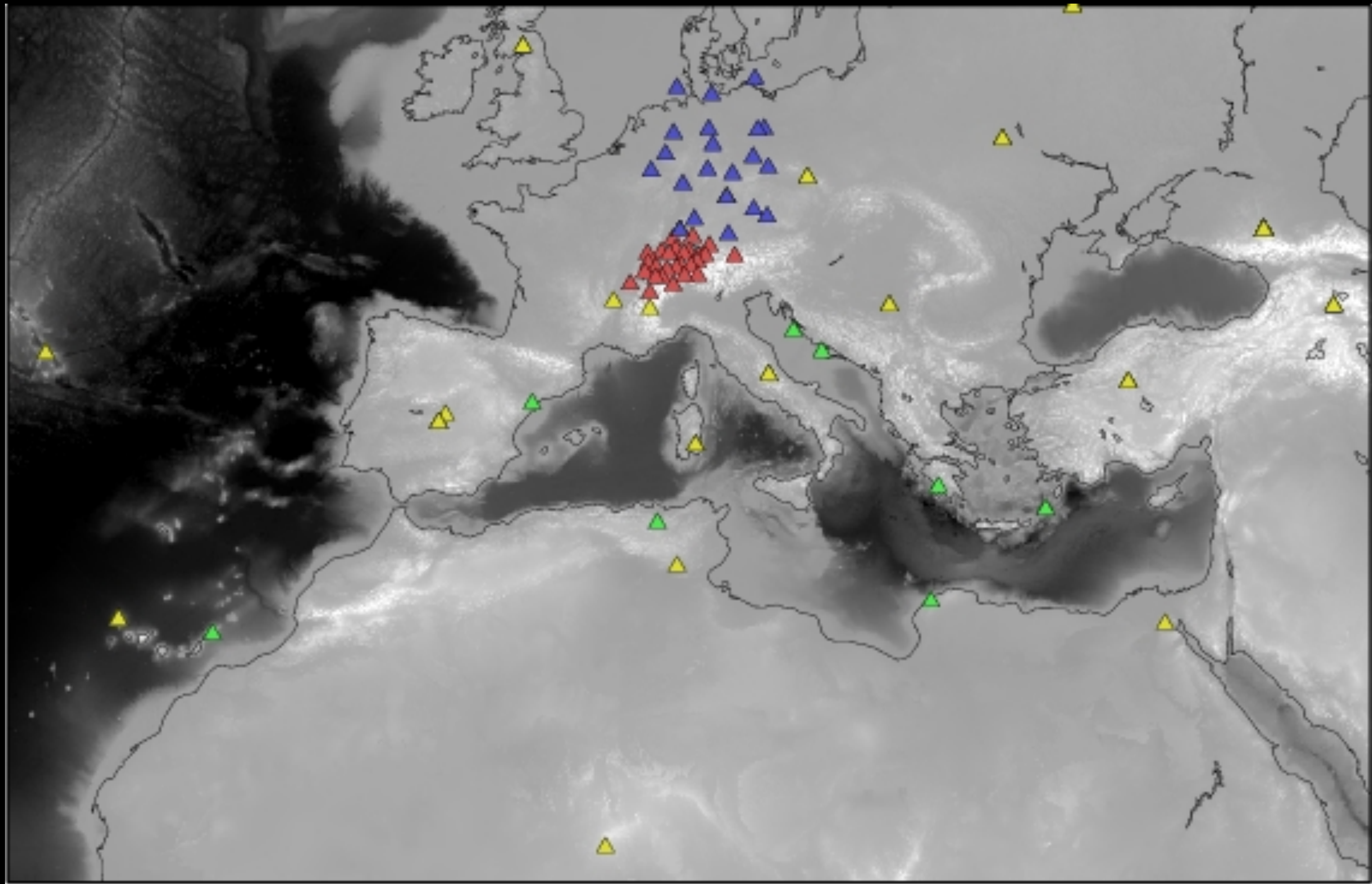

new model, global view

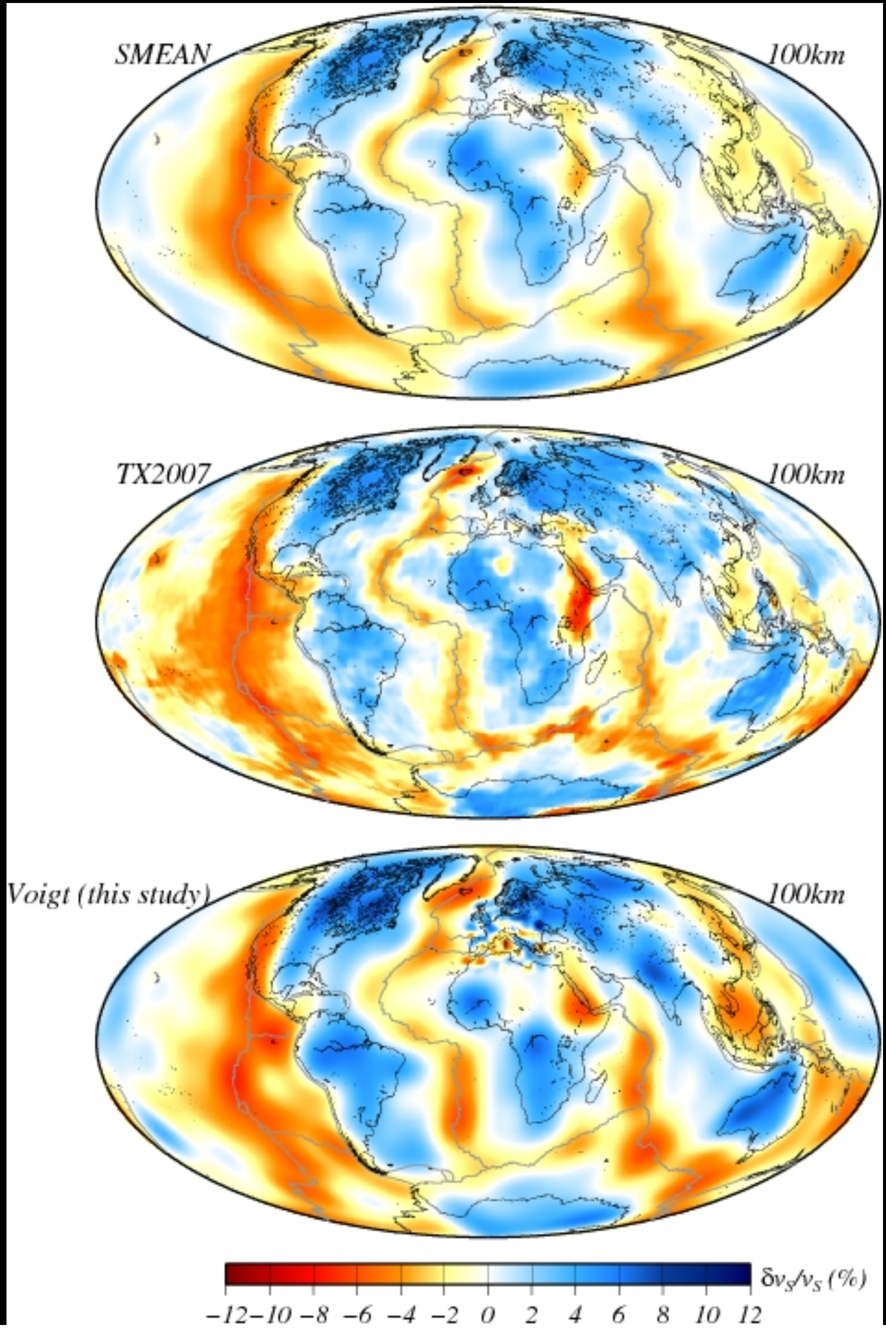

new model, continental-scale view

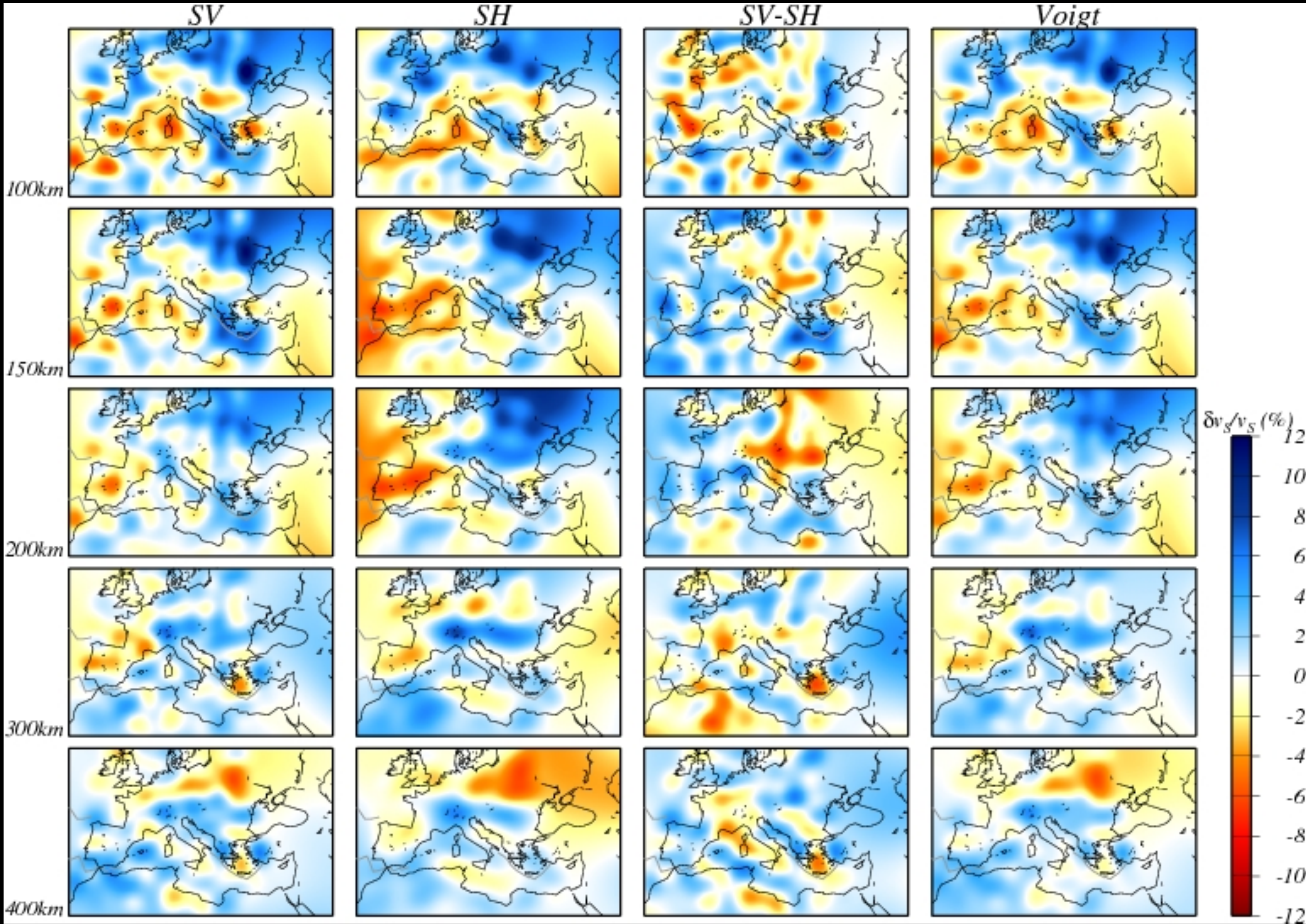

new model, vertical sections

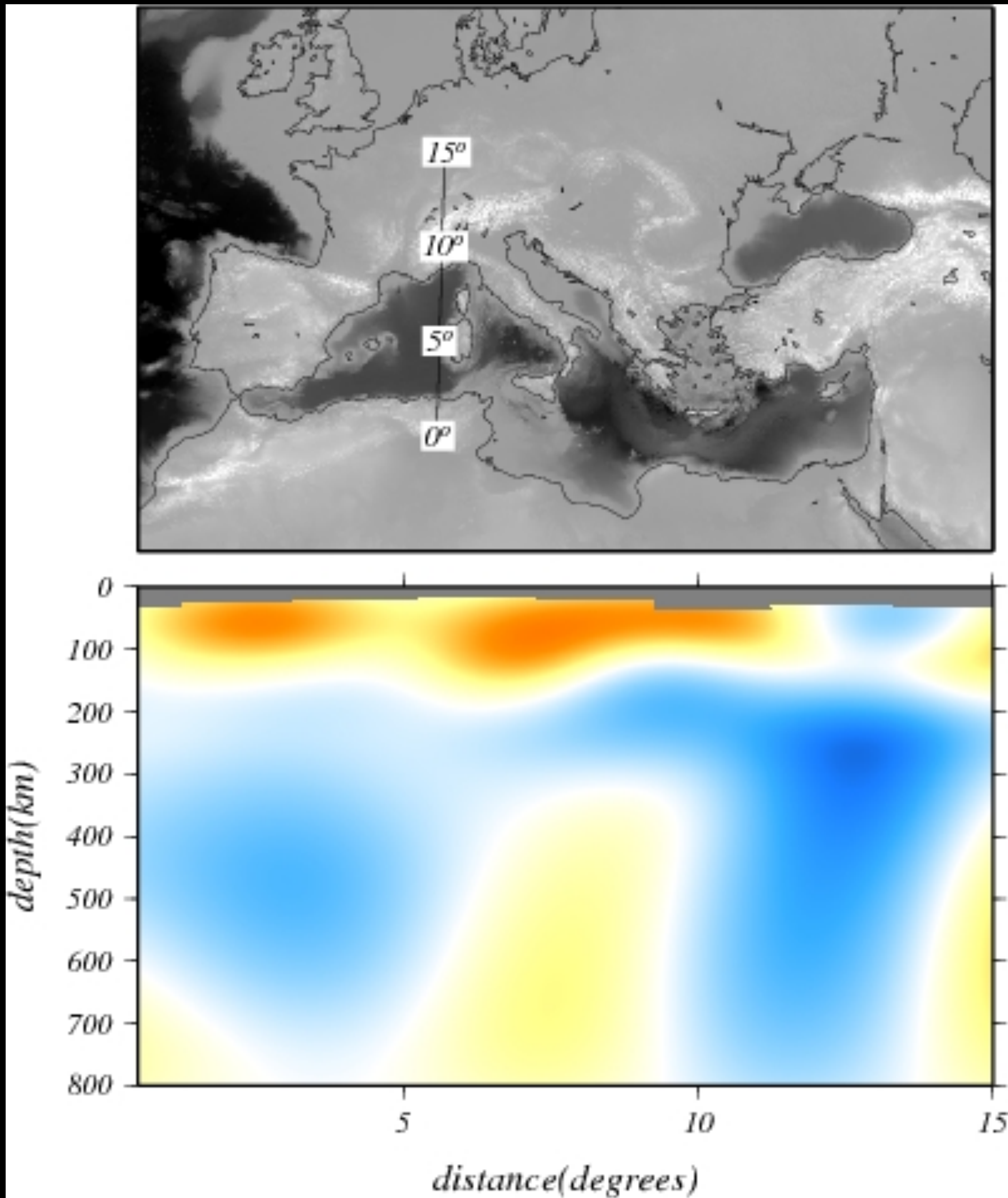

new model, vertical sections

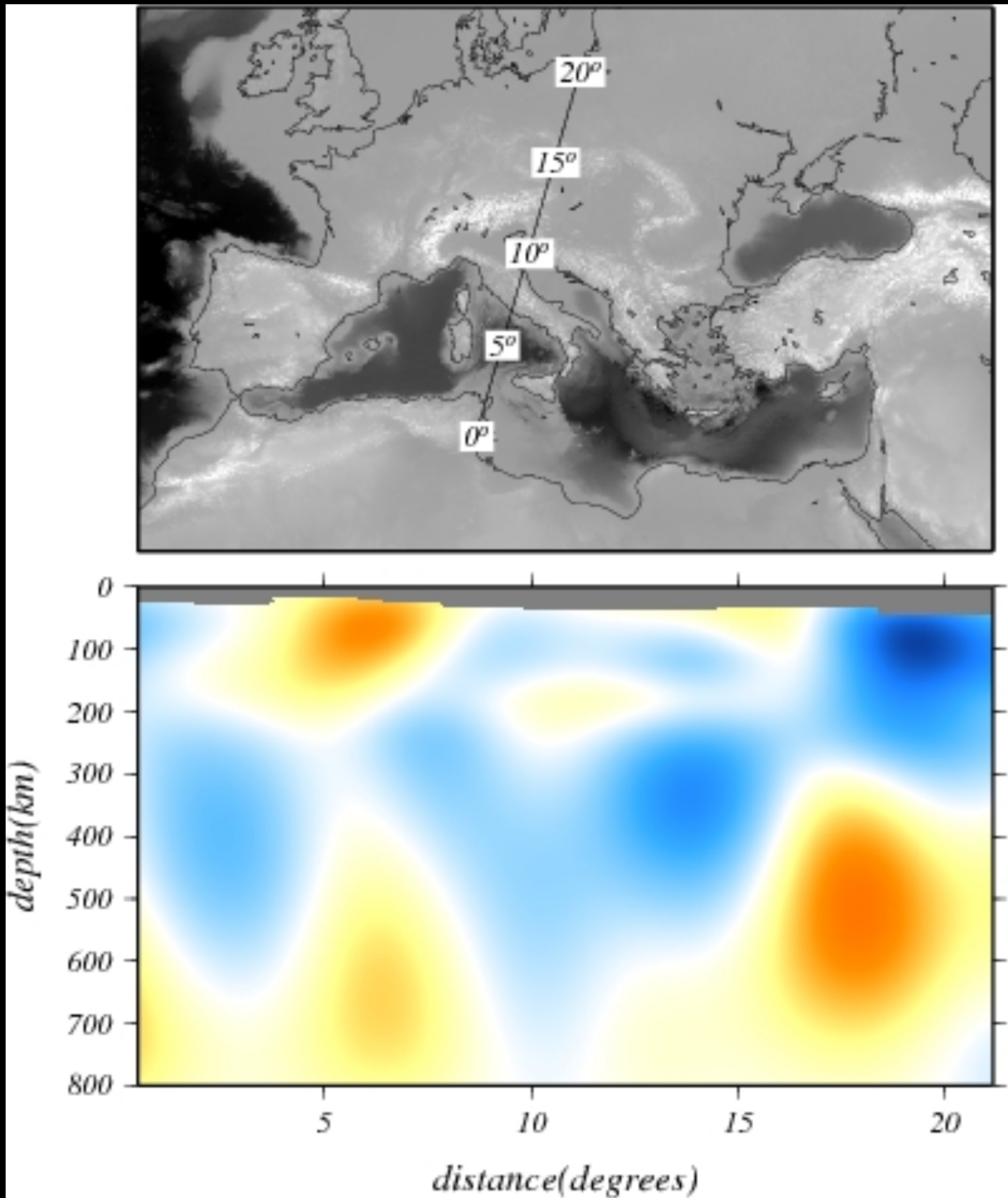

new model, vertical sections

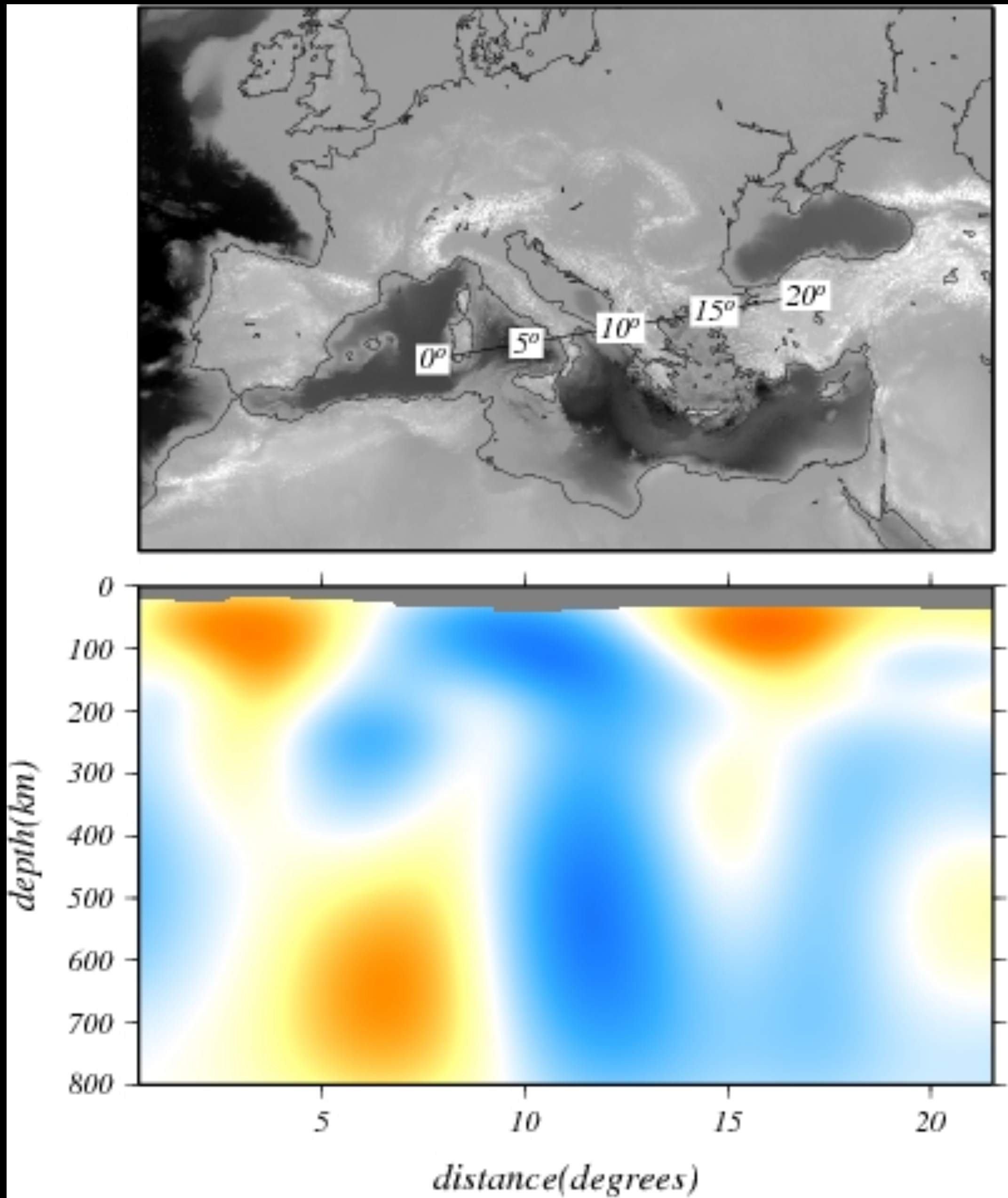

new model, vertical sections

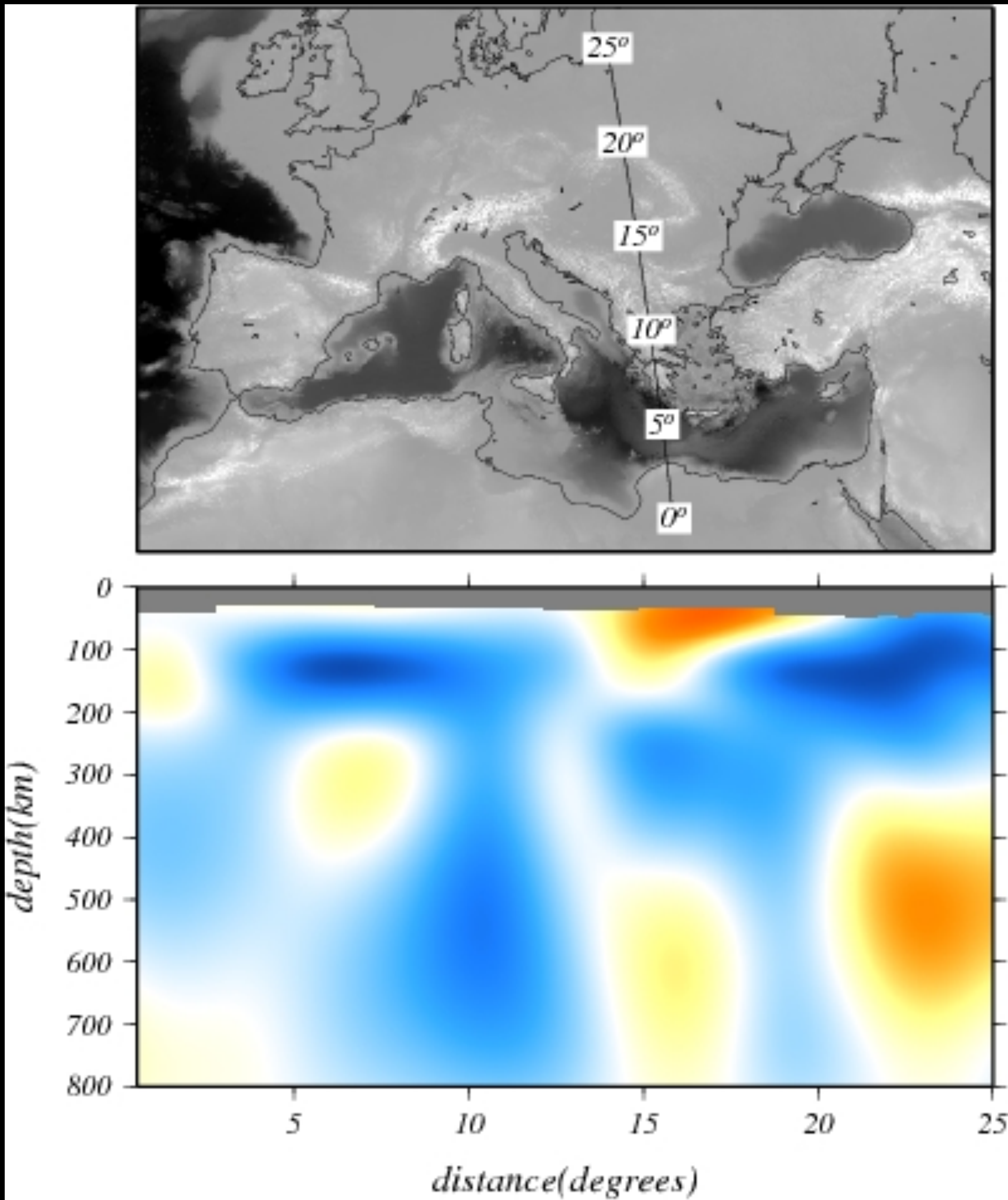

Comparison with body-wave tomography

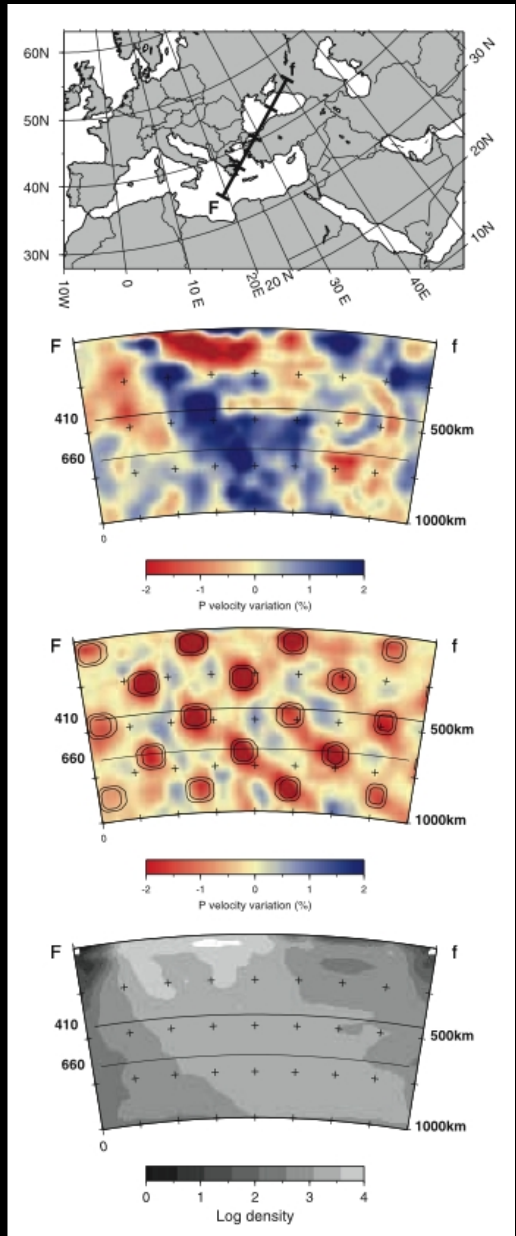

Piromallo & Morelli 2005

adaptive-resolution tomography

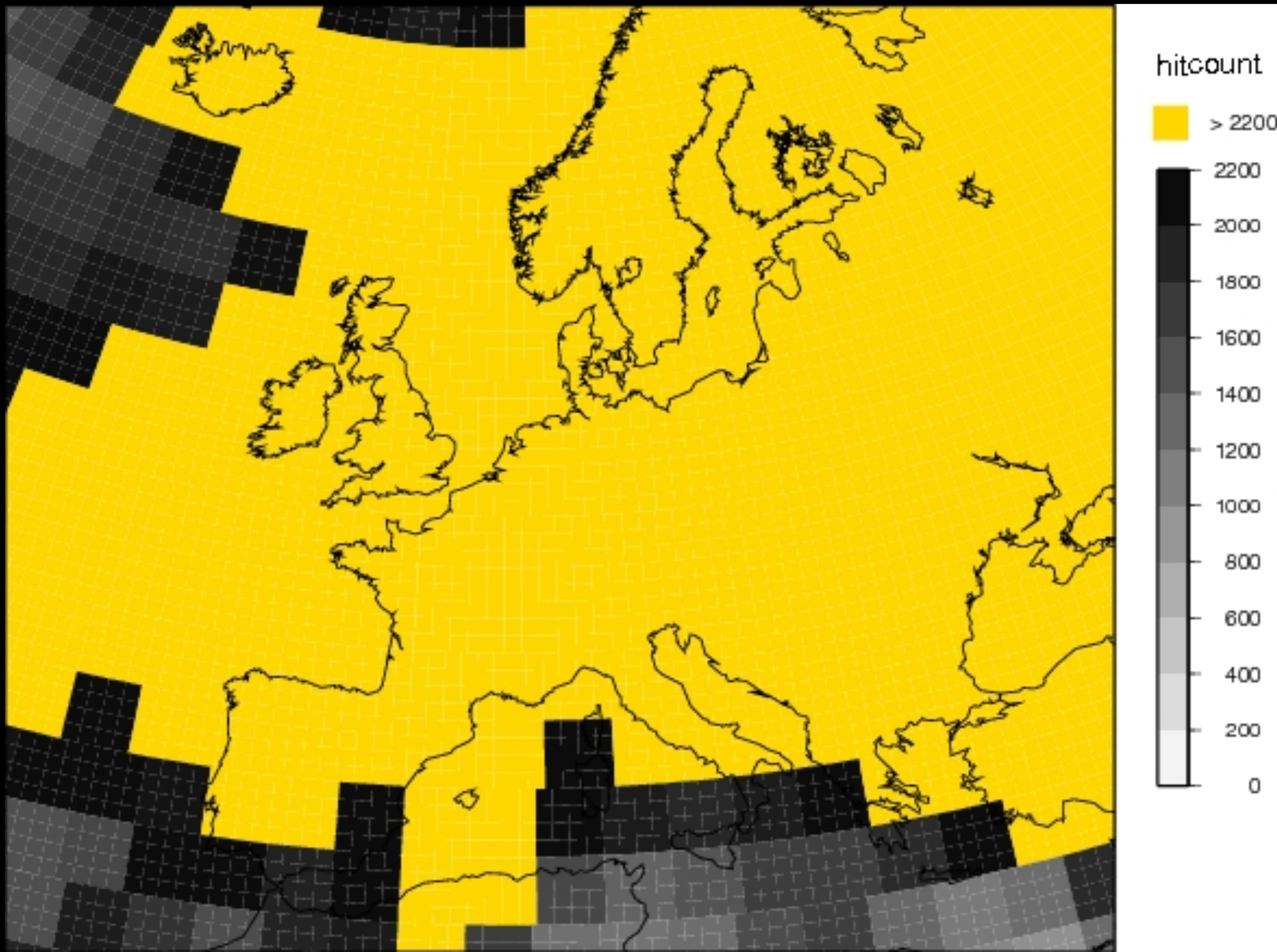

Julia Schäfer, 2009

adaptive-resolution tomography

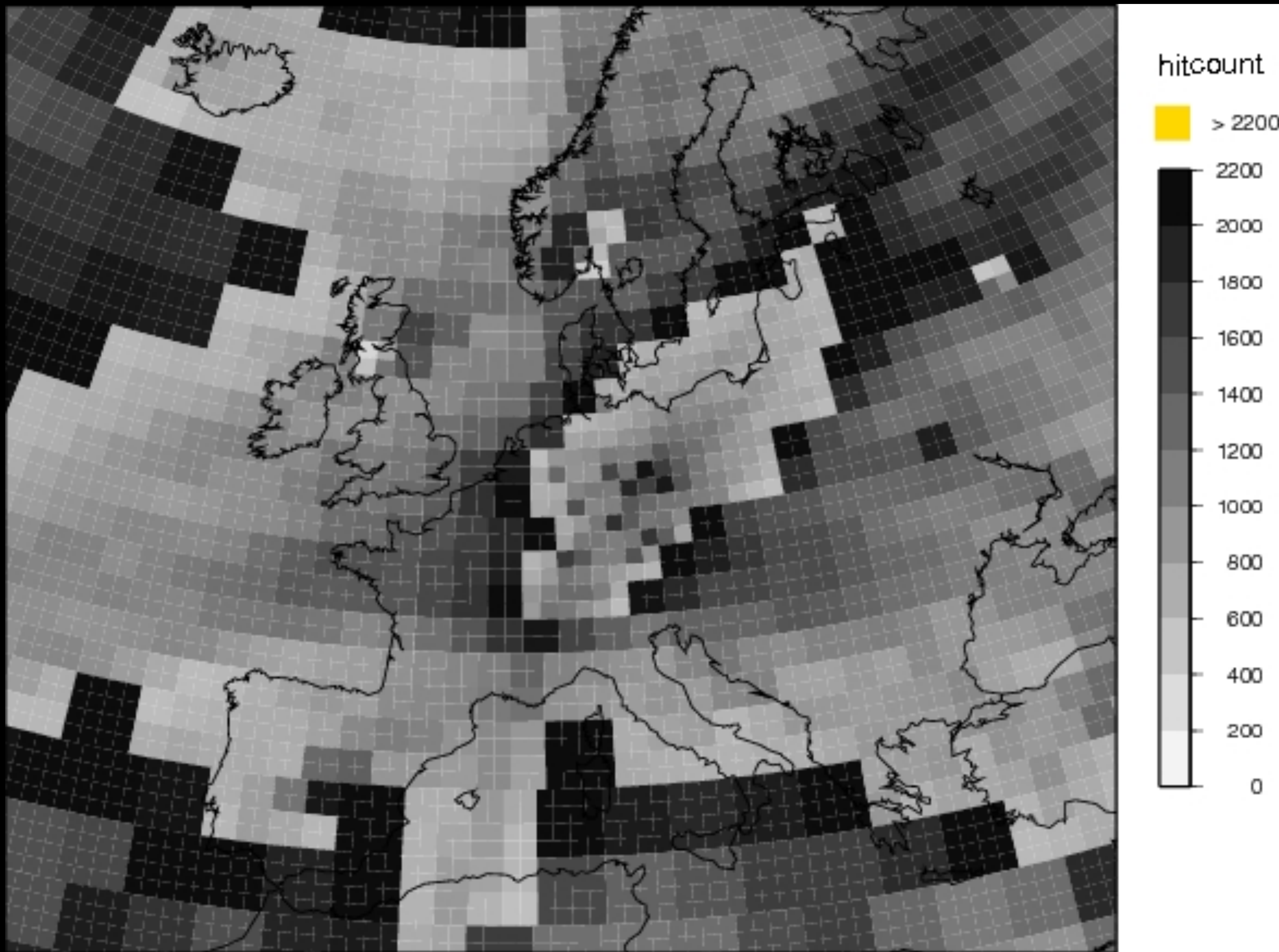

Julia Schäfer, 2009

adaptive-resolution tomography

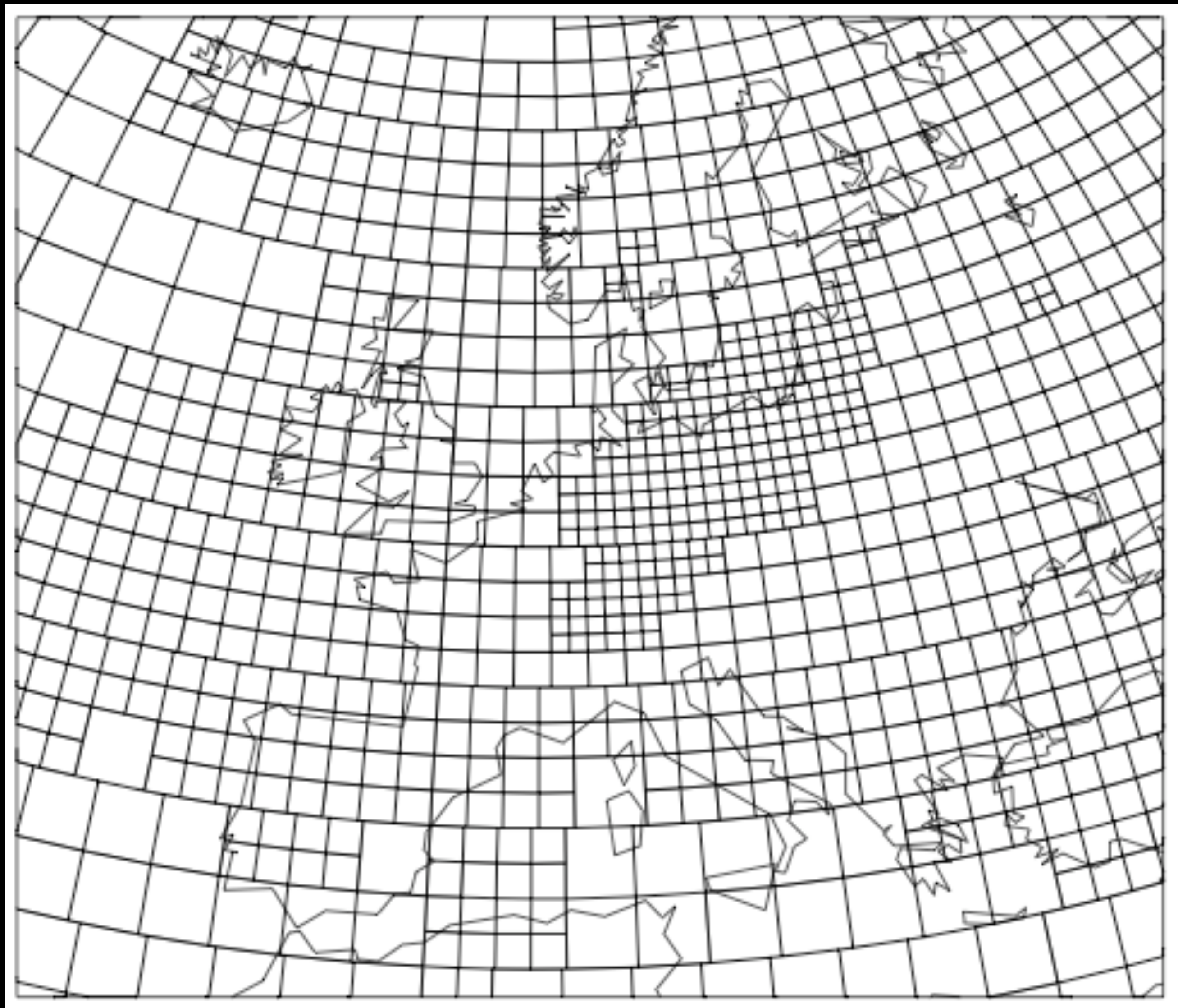

Julia Schäfer, 2009

Rayleigh 75s and thermal thickness of lithosphere

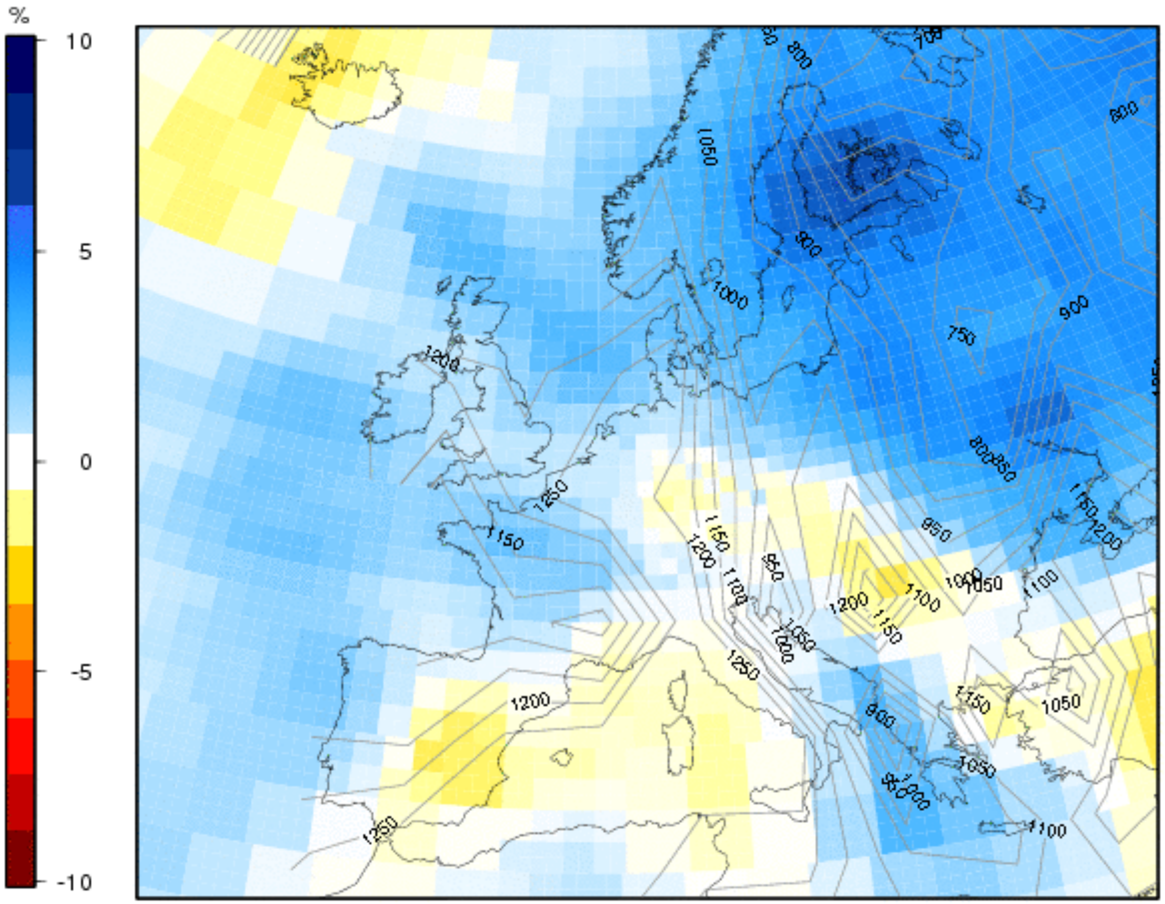

isolines represent temperature at 100 km depth
(geothermal data: TC 1, Artemieva, 2006)

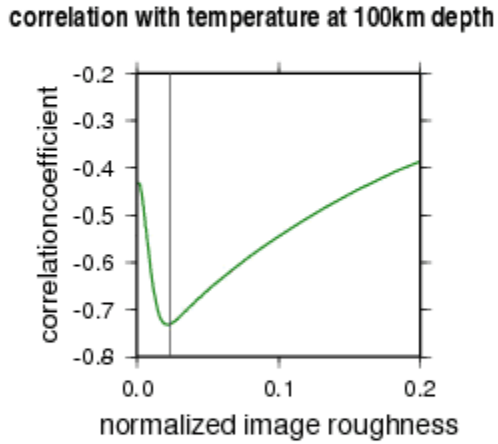

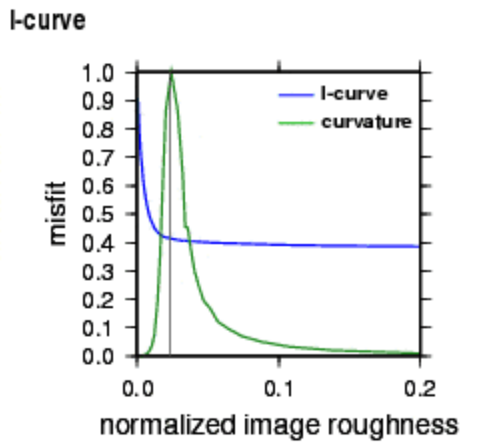

Schäfer, Boschi and Kissling, 2009

contribution from ambient noise data

teleseismic data | **ambient-noise data**

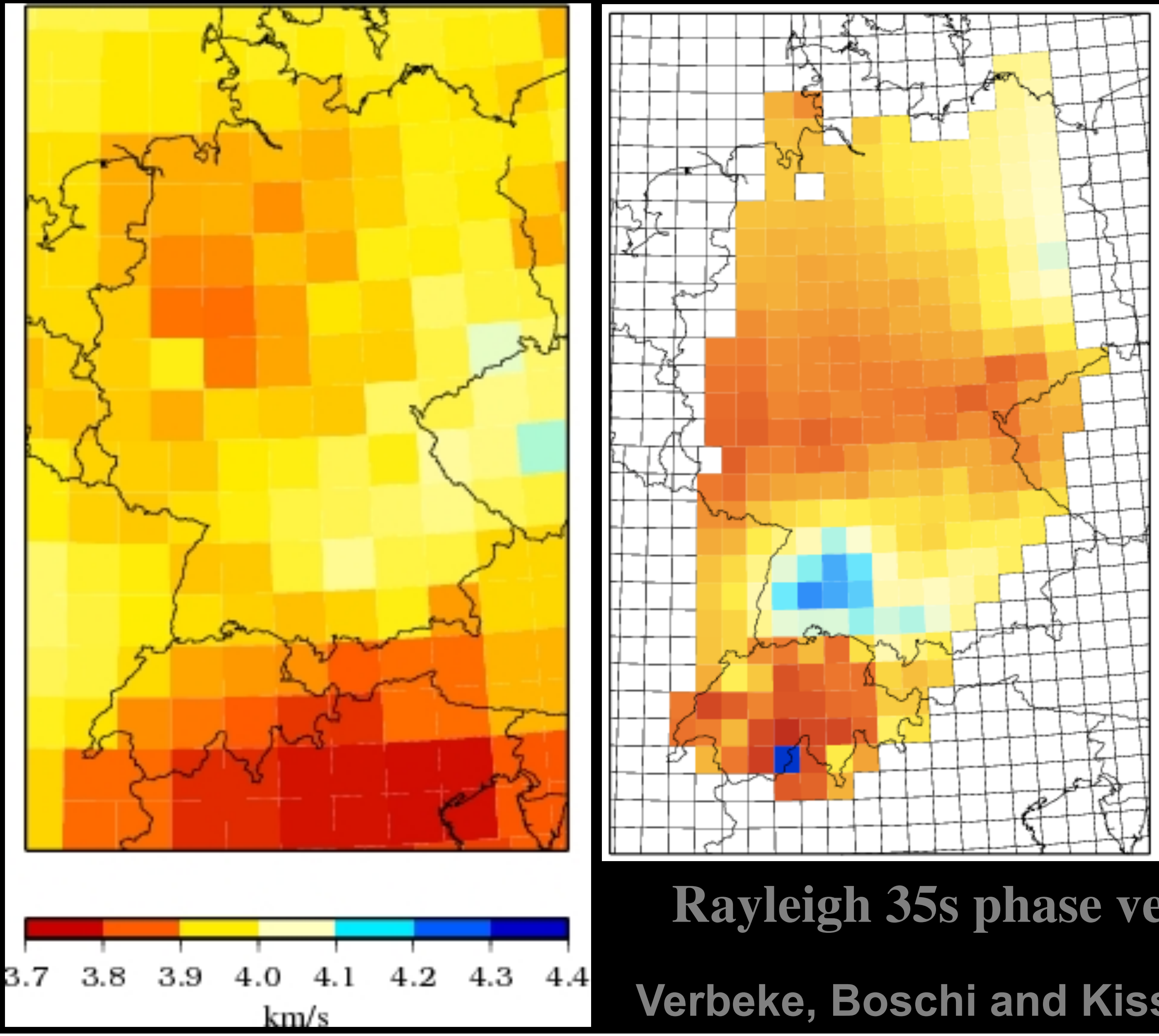

Rayleigh 35s phase velocity

Verbeke, Boschi and Kissling, 2009

S tomography (body waves)

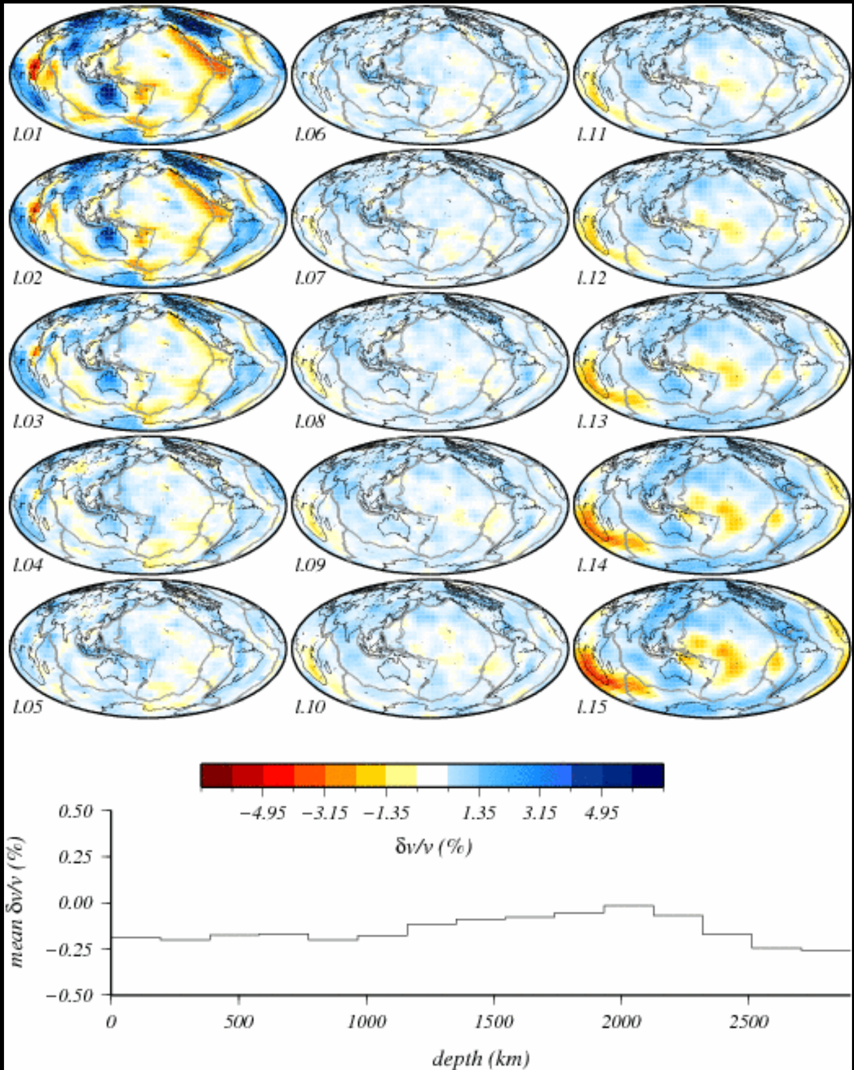

where should we put a discontinuity?

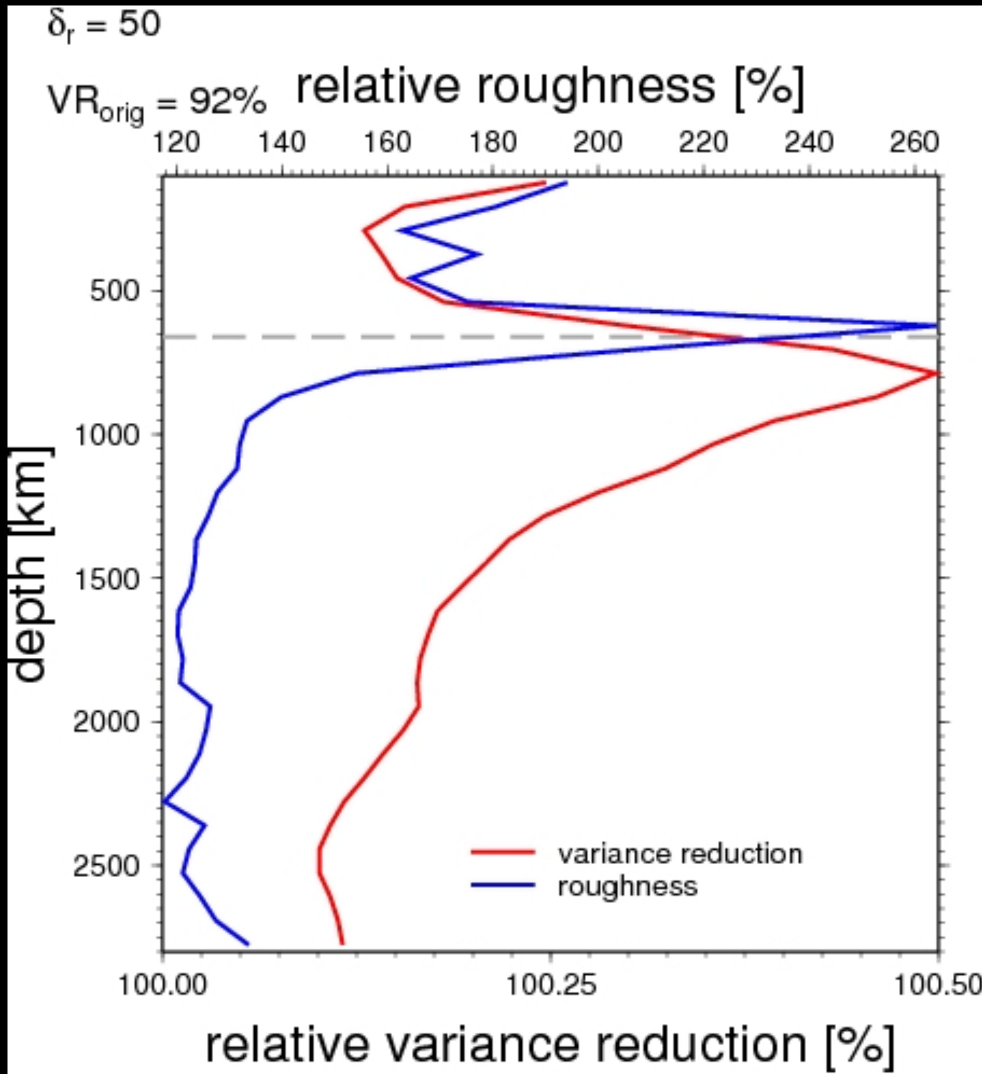

Becker and Boschi, 2009

new body wave model compared to published ones

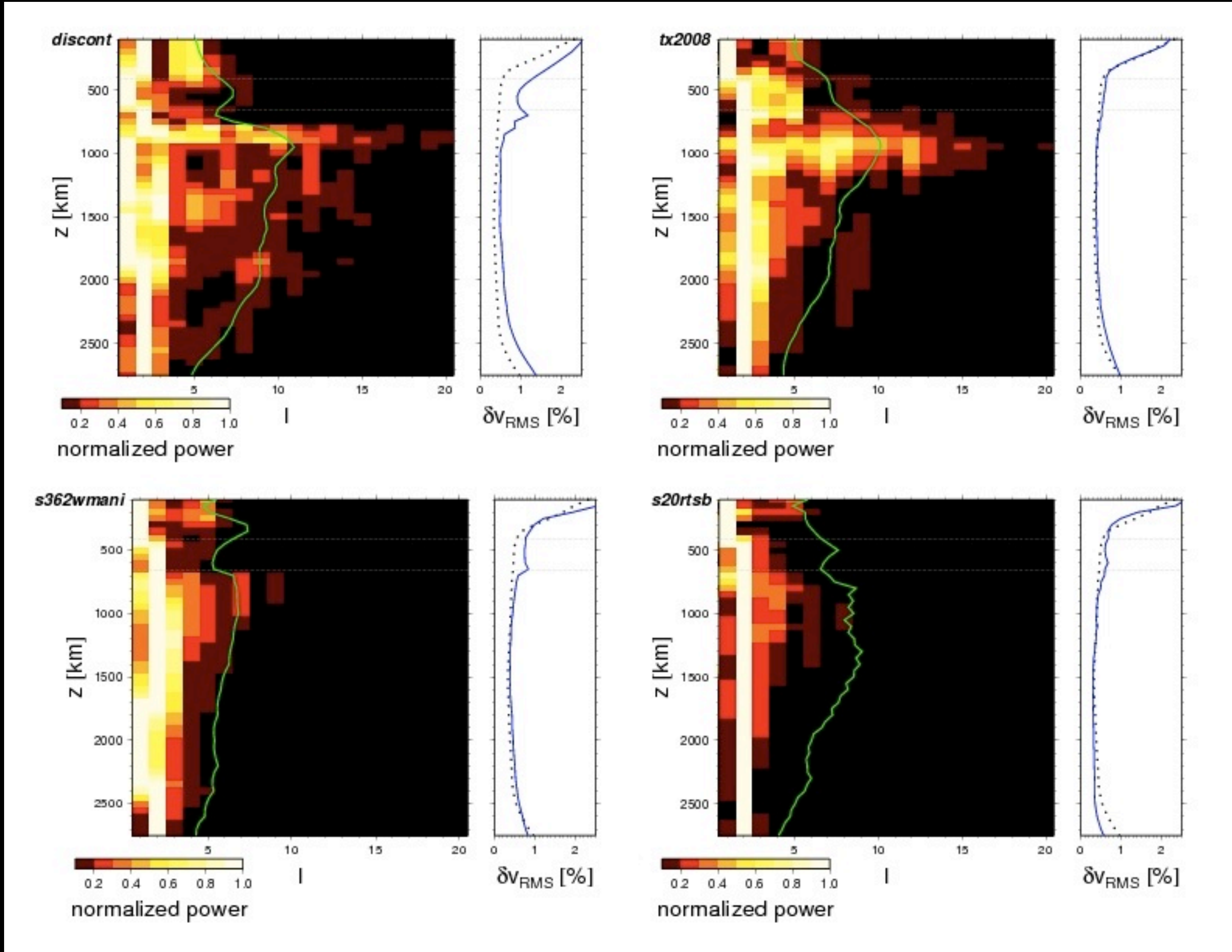

S waves and Love/Rayleigh fundamental mode

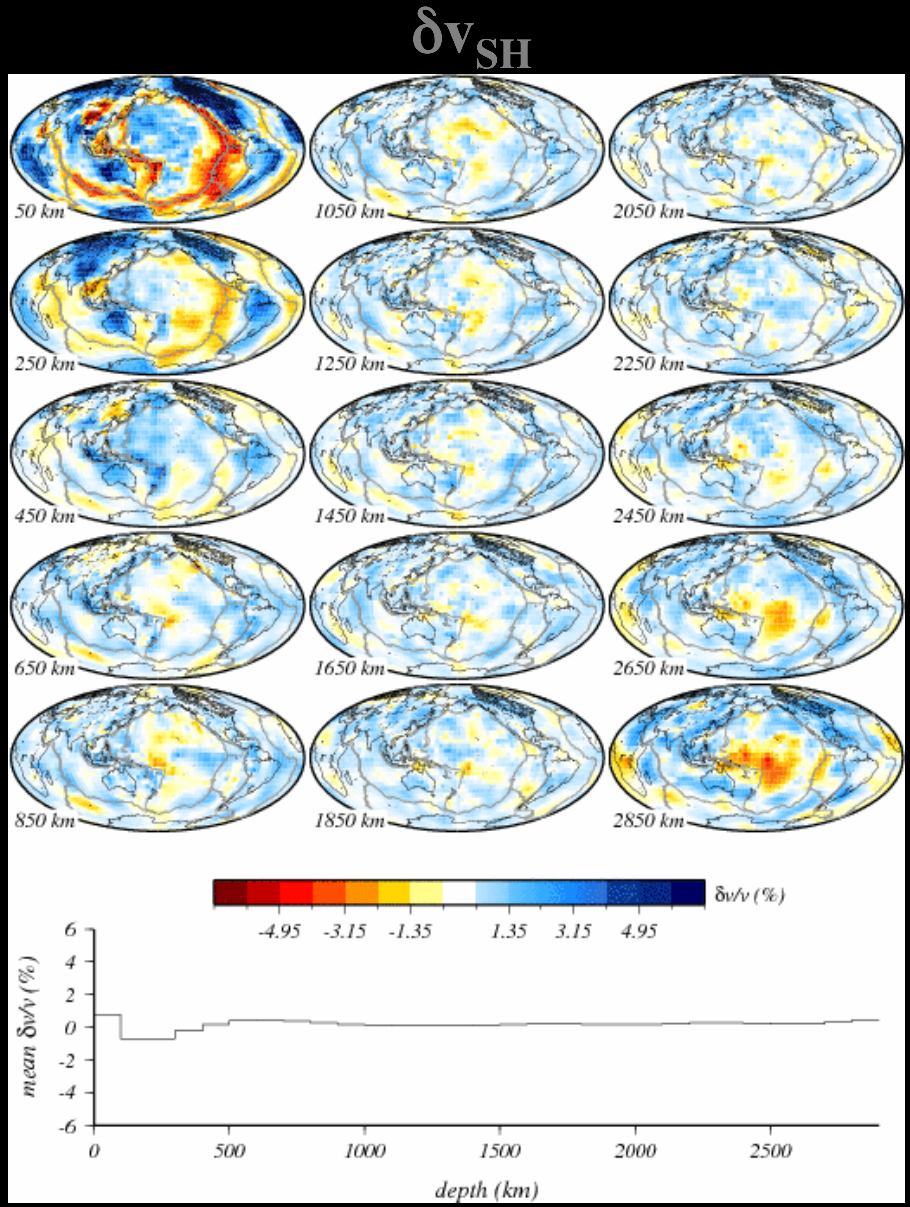

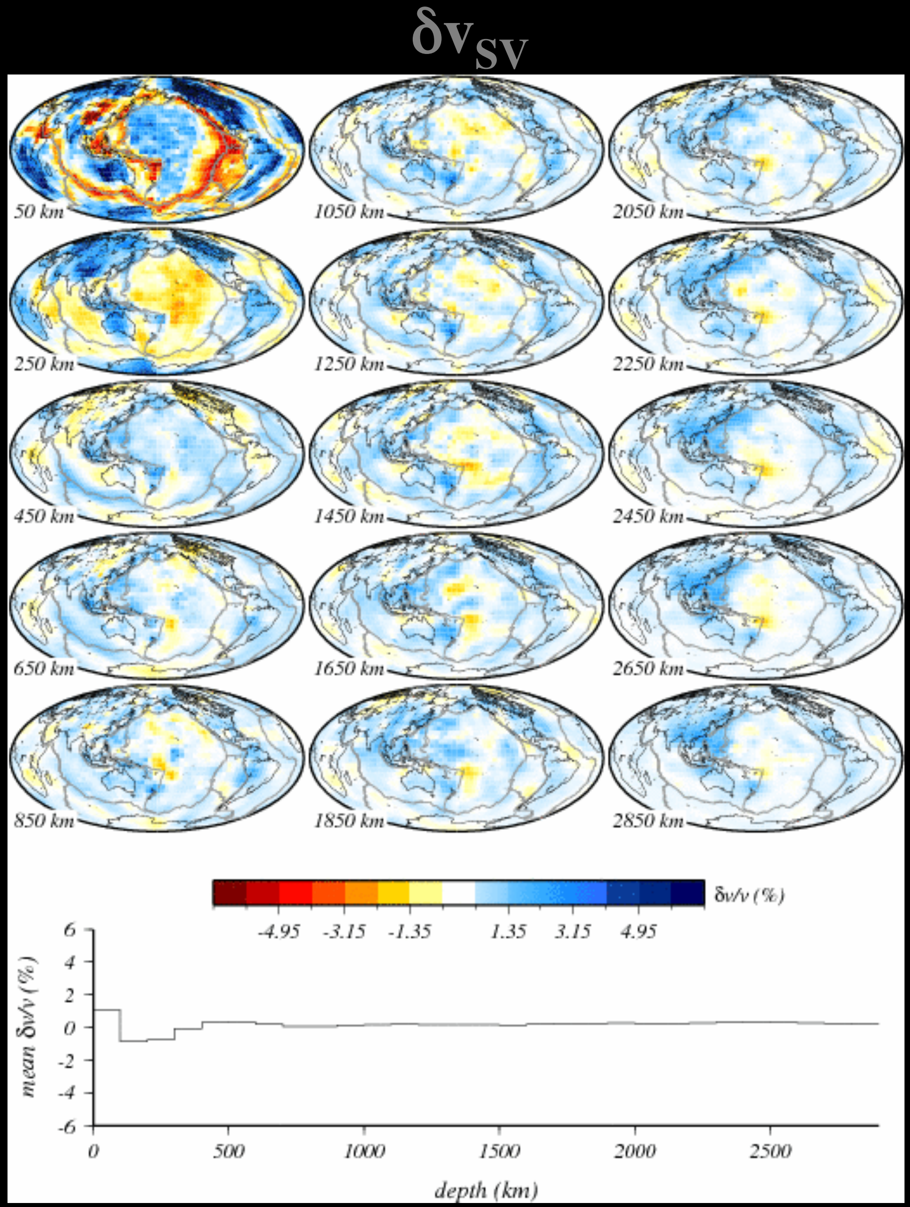

collaborators: Becker, Ekström, Gu, van Heijst, Houser, Trampert, Simmons

S waves and Love/Rayleigh modes up to 6th overtone

δv_{SH}

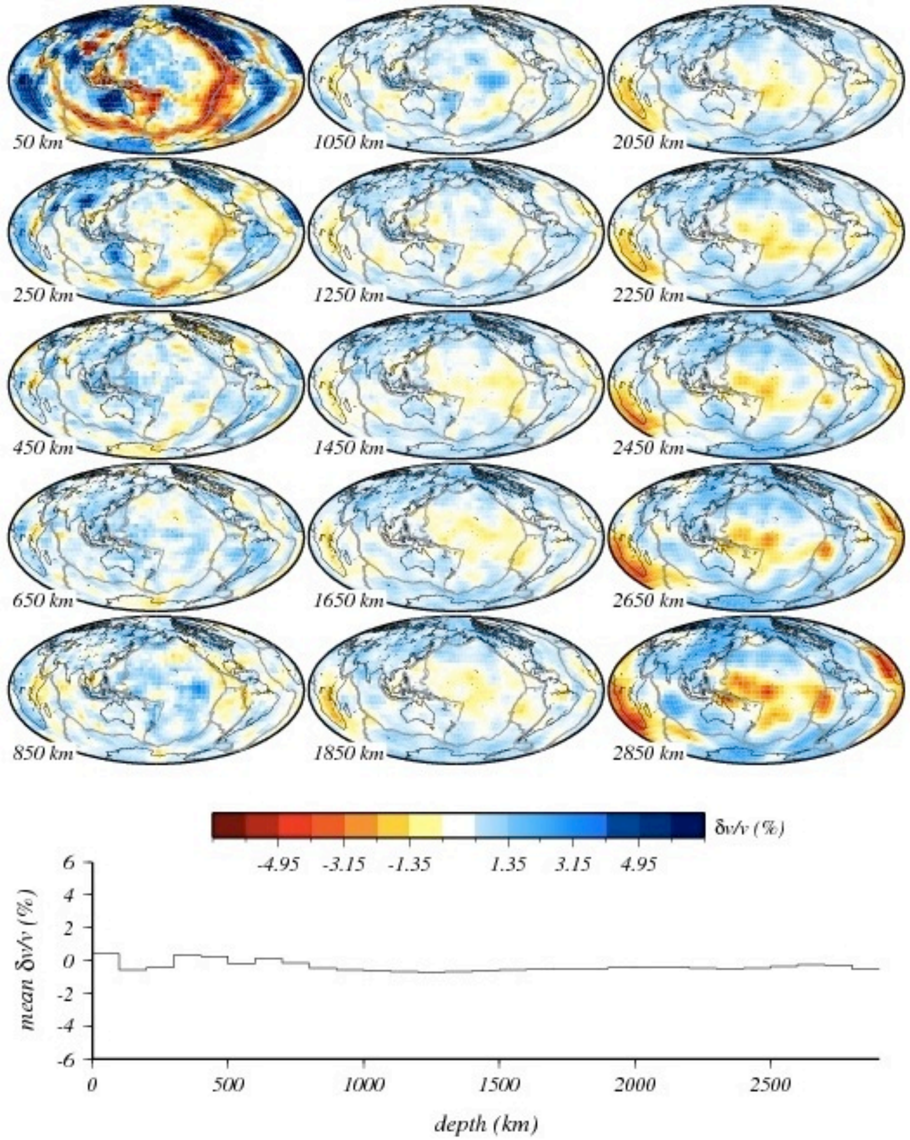

δv_{SV}

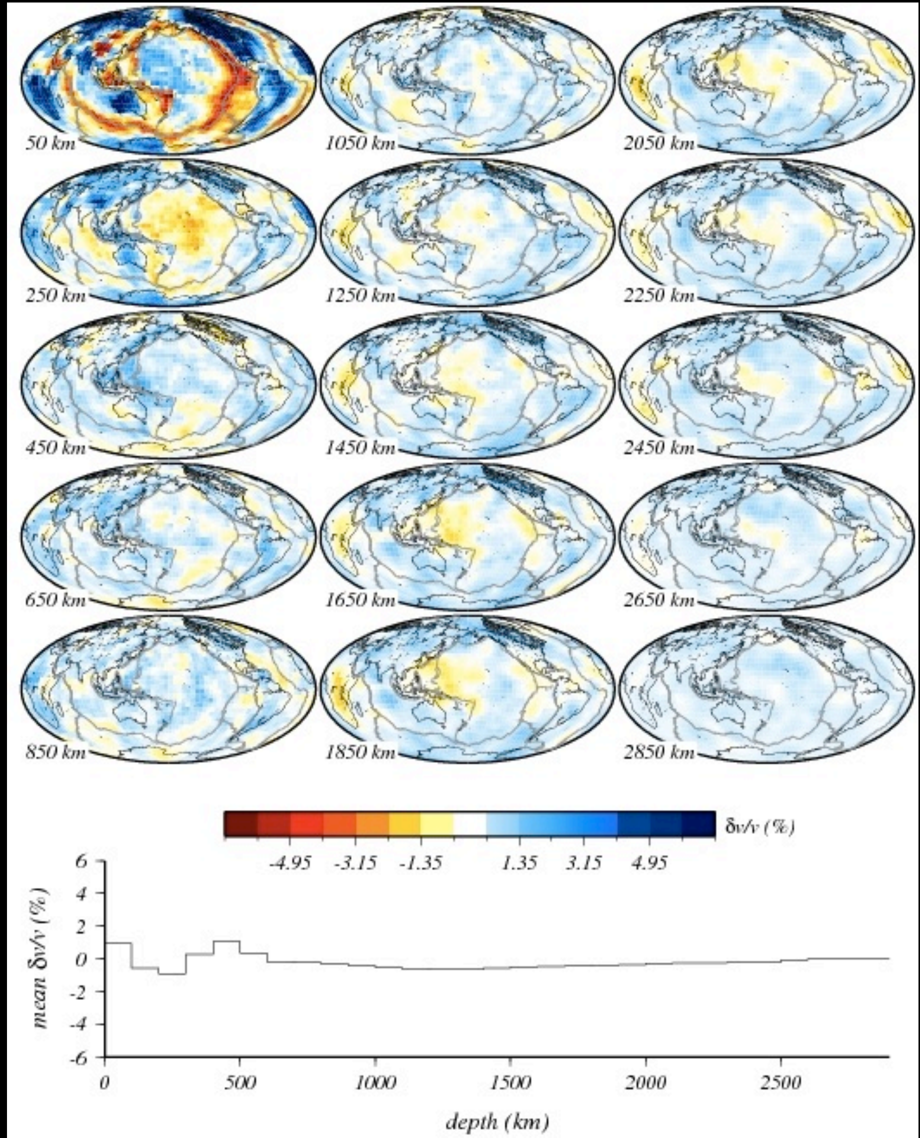

collaborators: Becker, Ekström, Gu, van Heijst, Houser, Trampert, Simmons

summary

1. **mapped slabs are globally correlated with expected ones**
2. **mapped slow anomalies are correlated with advected plume distribution, limited to mantle under Africa and central Pacific**
3. **the next step to better understand the transition zone is to combine body and surface waves, including overtones**
4. **the next step in surface-wave tomography is to identify models that explain both ambient-noise and teleseismic data.**

4. five slides on finite-frequency tomography

Trade-off between model complexity and data-fit as a criterion for model selection

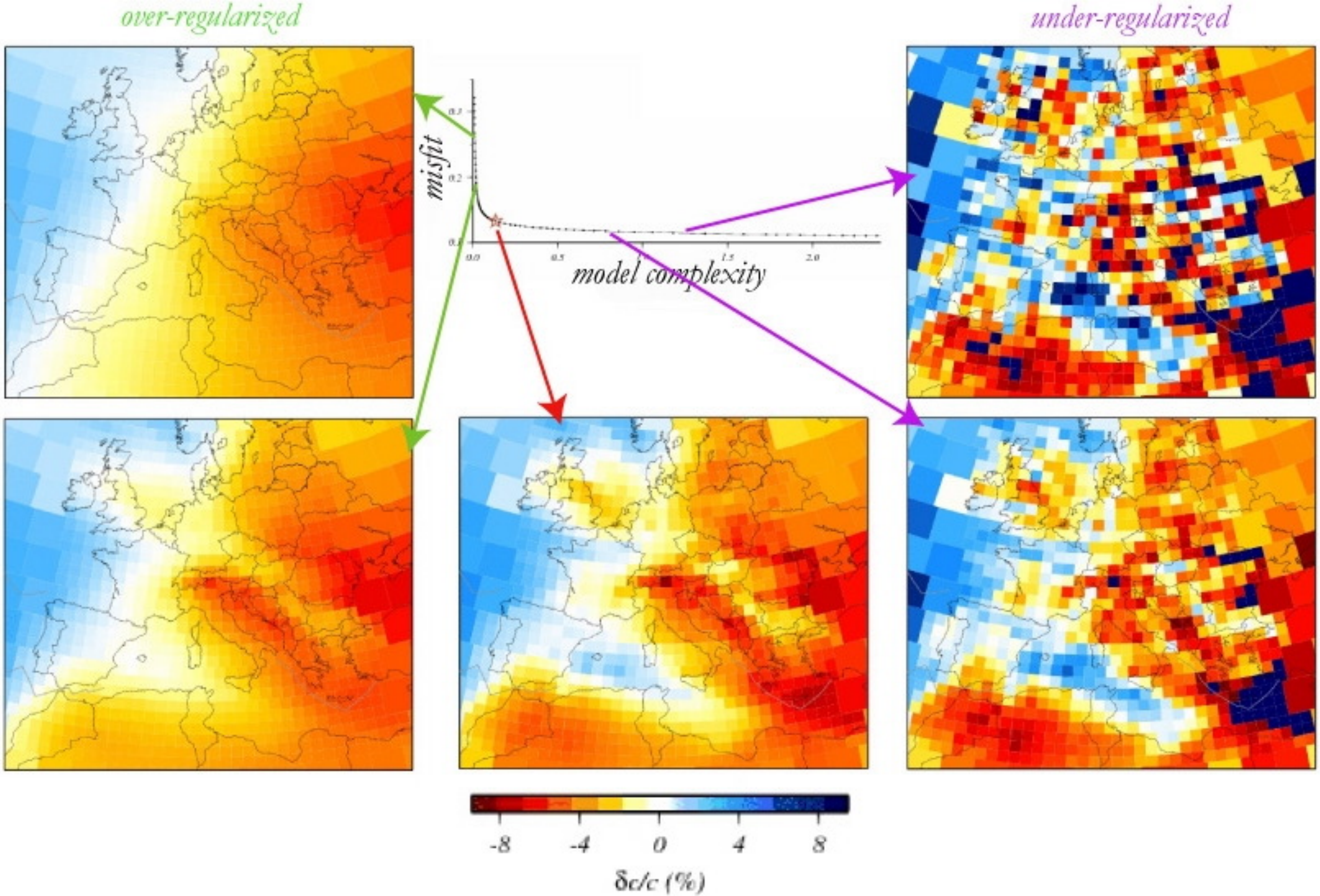

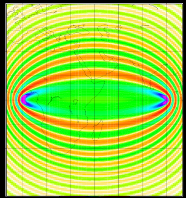

Sensitivity kernels: how they look like

Love waves, 150 s period. Source and receiver on the equator, 90° apart. Reference model is PREM.

adjoint method (membrane waves)

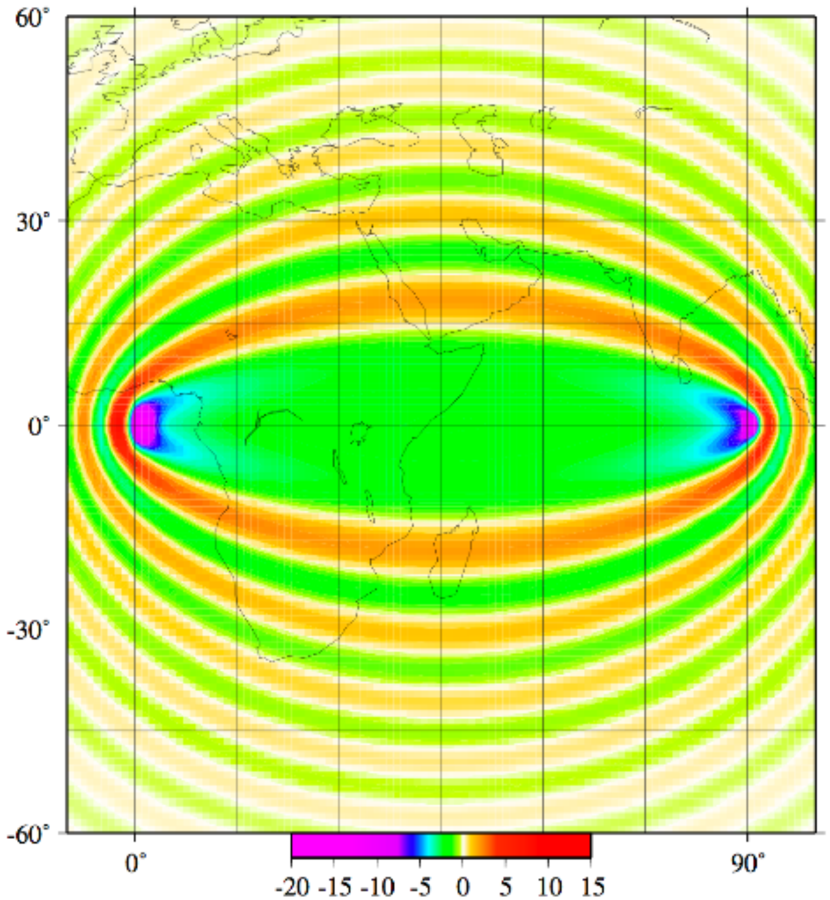

analytical kernel from e.g. Spetzler et al. (2002)

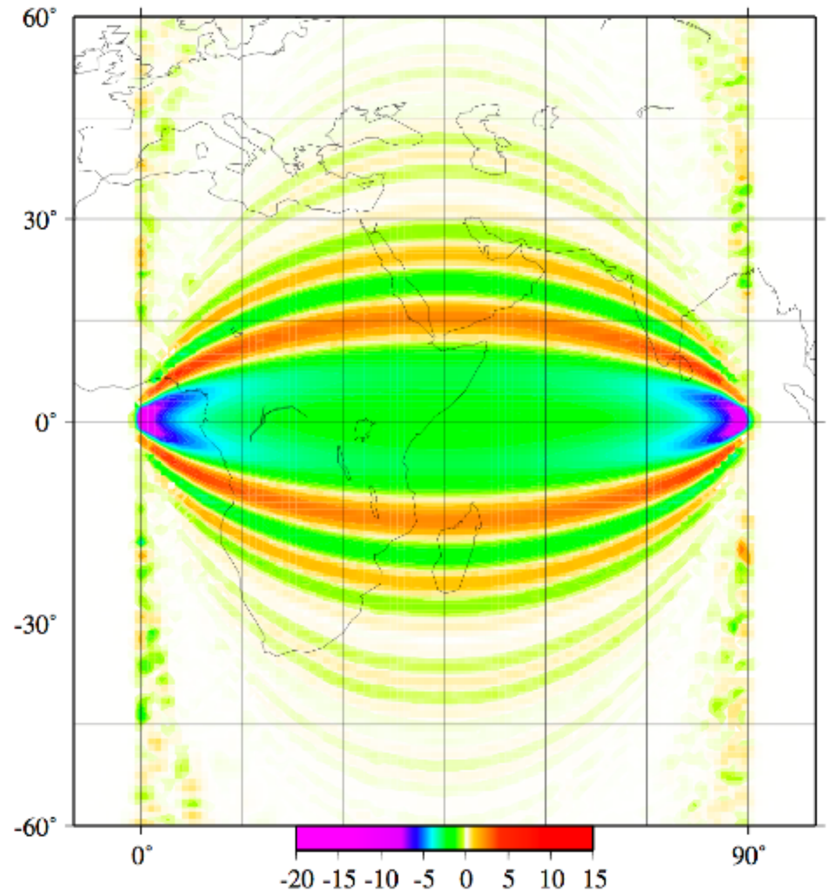

“benchmark” test: long spatial wavelength anomalies

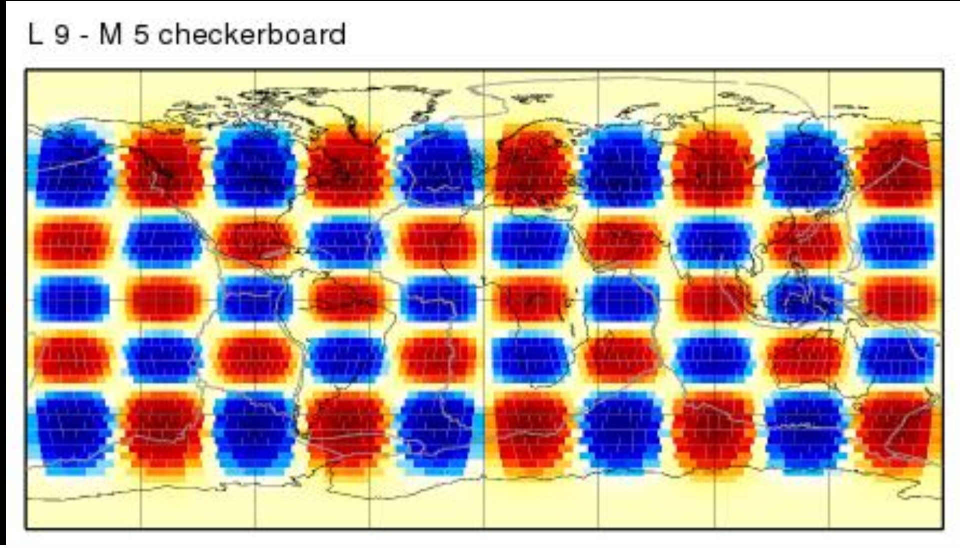

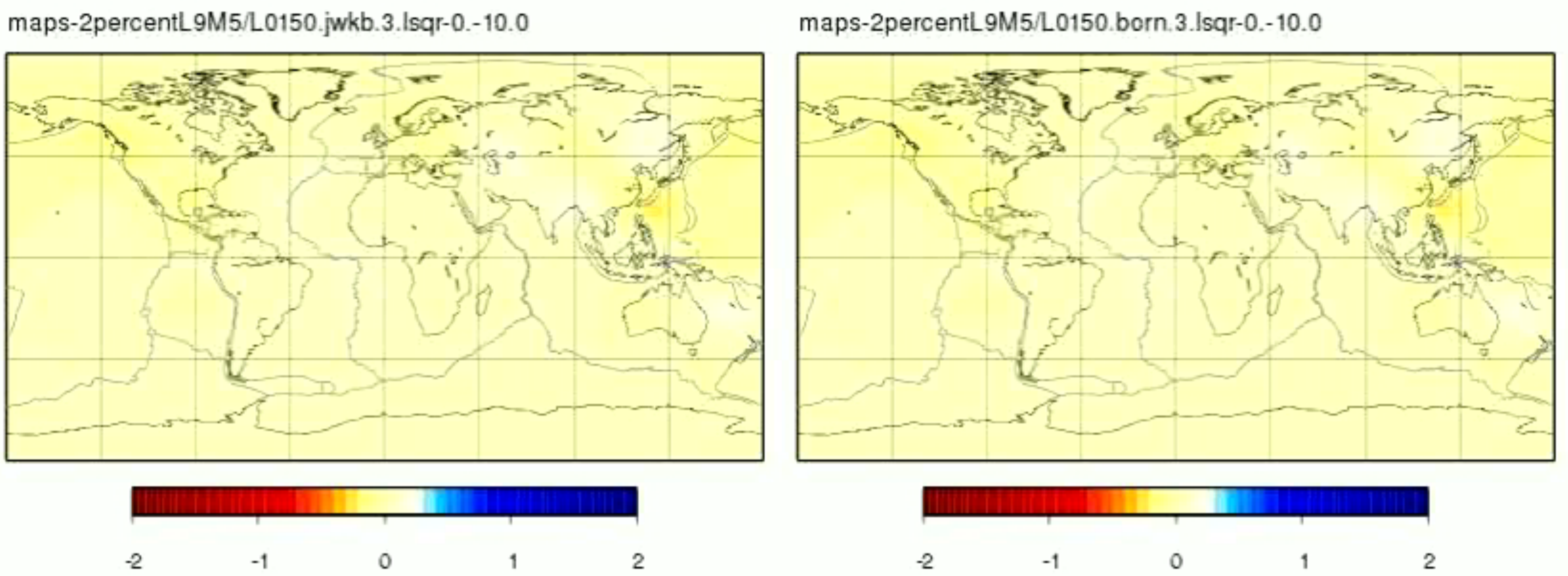

Peter, Boschi & Woodhouse, 2008

“benchmark” test: shorter spatial wavelength anomalies

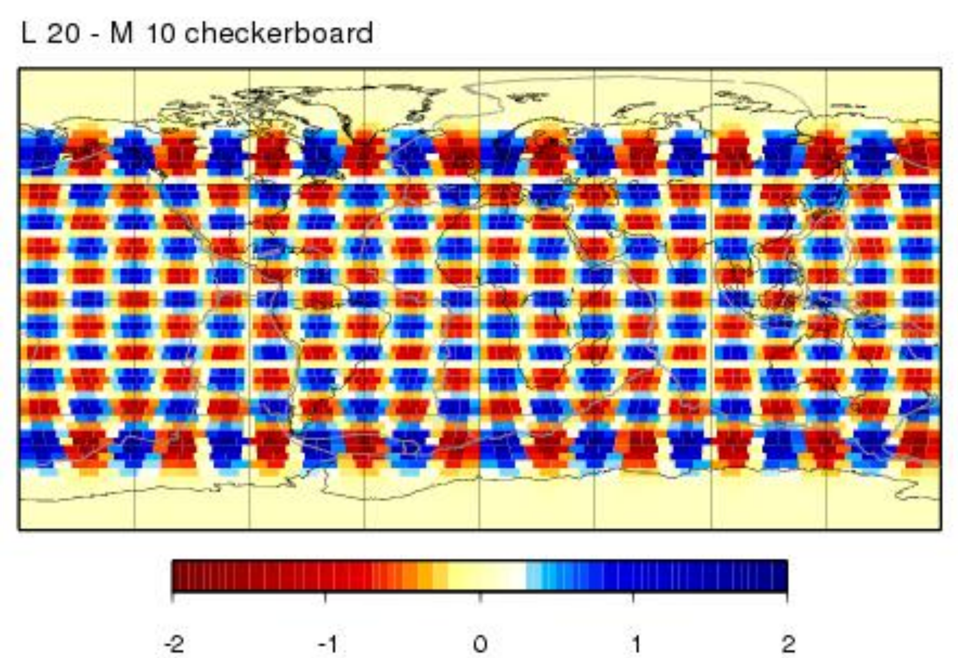

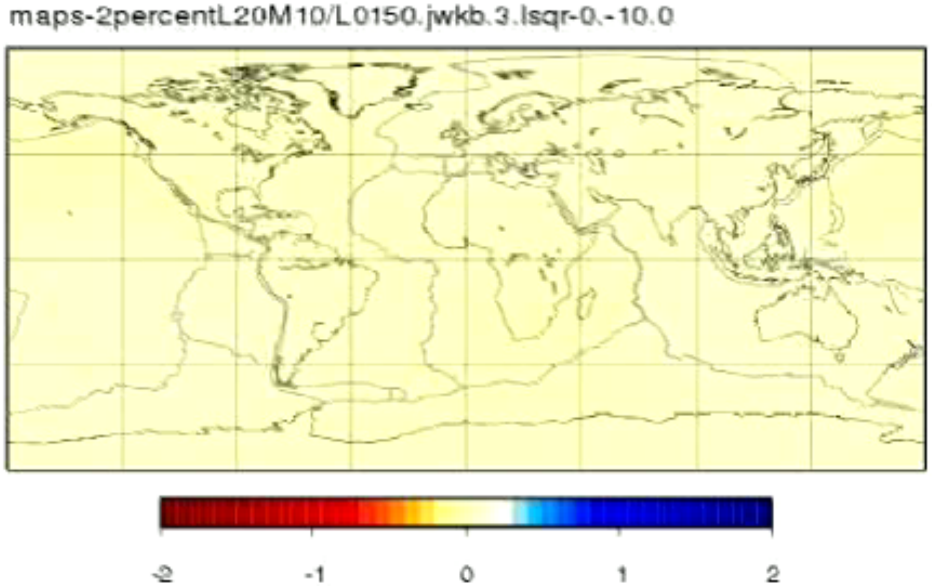

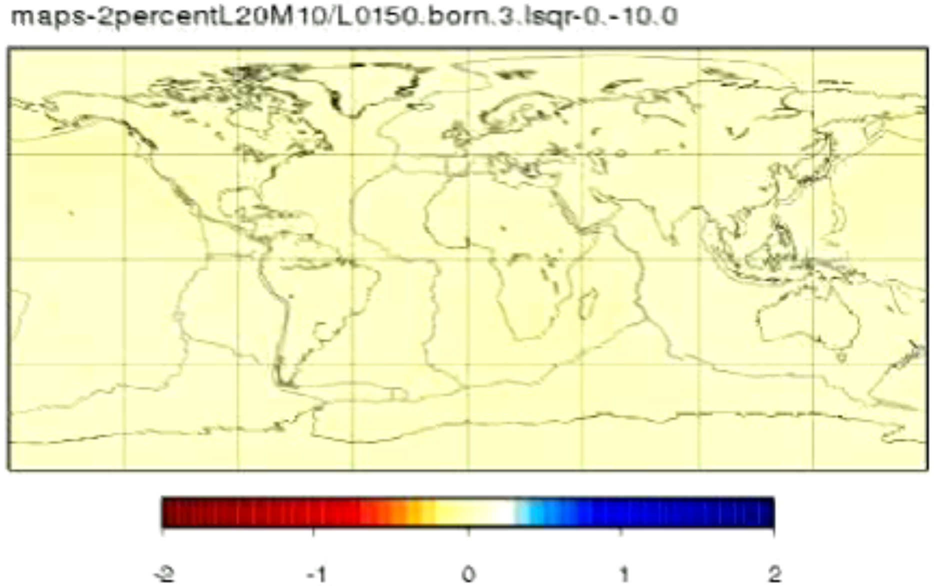

Peter, Boschi & Woodhouse, 2008

“benchmark” test: realistic “input” model

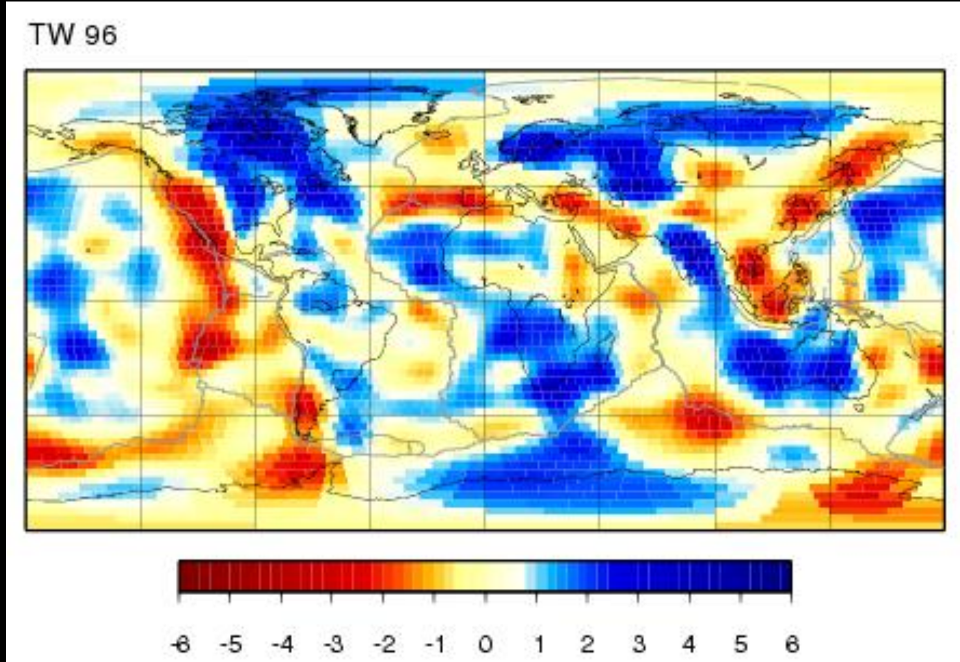

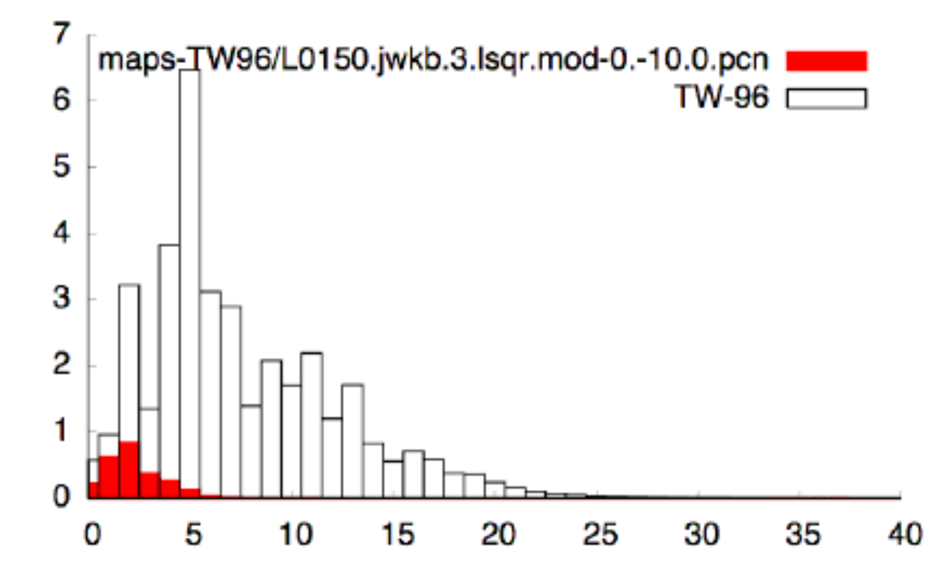

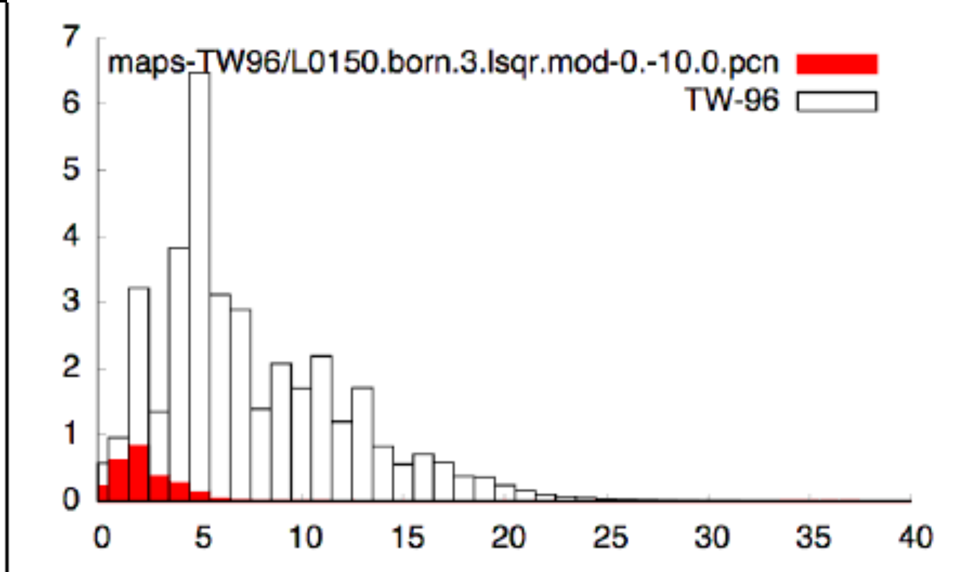

Peter, Boschi & Woodhouse, 2008